Ollscoil na Gaillimhe
University of Galway

Provided by the author(s) and University of Galway in accordance with publisher policies. Please cite the published version when available.

Title	Developing detailed chemical kinetic mechanisms for fuel combustion
Author(s)	Curran, Henry J.
Publication Date	2018-07-01
Publication Information	Curran, Henry J. (2019). Developing detailed chemical kinetic mechanisms for fuel combustion. Proceedings of the Combustion Institute, 37(1), 57-81. doi: https://doi.org/10.1016/j.proci.2018.06.054
Publisher	Elsevier
Link to publisher's version	https://doi.org/10.1016/j.proci.2018.06.054
Item record	http://hdl.handle.net/10379/15121
DOI	http://dx.doi.org/10.1016/j.proci.2018.06.054

Downloaded 2024-04-27T08:37:11Z

Some rights reserved. For more information, please see the item record link above.

Developing detailed chemical kinetic mechanisms for fuel combustion

Henry J. Curran

[1]Combustion Chemistry Centre, National University of Ireland, Galway, Ireland

Abstract

This paper discusses a brief history of chemical kinetic modeling, with some emphasis on the development of chemical kinetic mechanisms describing fuel oxidation. At high temperatures, the important reactions tend to be those associated with the H_2/O_2 and C_1–C_2 sub-mechanisms, particularly for non-aromatic fuels. At low temperatures, and for aromatic fuels, the reactions that dominate and control the reaction kinetics are those associated with the parent fuel and its daughter radicals. Strategies used to develop and optimize chemical kinetic mechanisms are discussed and some reference is made to lumped and reduced mechanisms. The importance of accurate thermodynamic parameters for the species involved is also highlighted, as is the little-studied importance of collider efficiencies of different third bodies involved in pressure-dependent reactions.

1. Introduction

Combustion is the ultimate interdisciplinary field; it requires knowledge of chemistry, physics, fluid dynamics, thermodynamics, mathematics and computer science. In addition, combustion science has a well-defined purpose in society today, facilitating the study and analysis of problems associated with the generation of air pollutants. Fig. 1 presents a diagram of the layers of information required to fully understand the combustion of a fuel from a molecular level leading ultimately to their use in modern combustors with increased efficiency and reduced emissions.

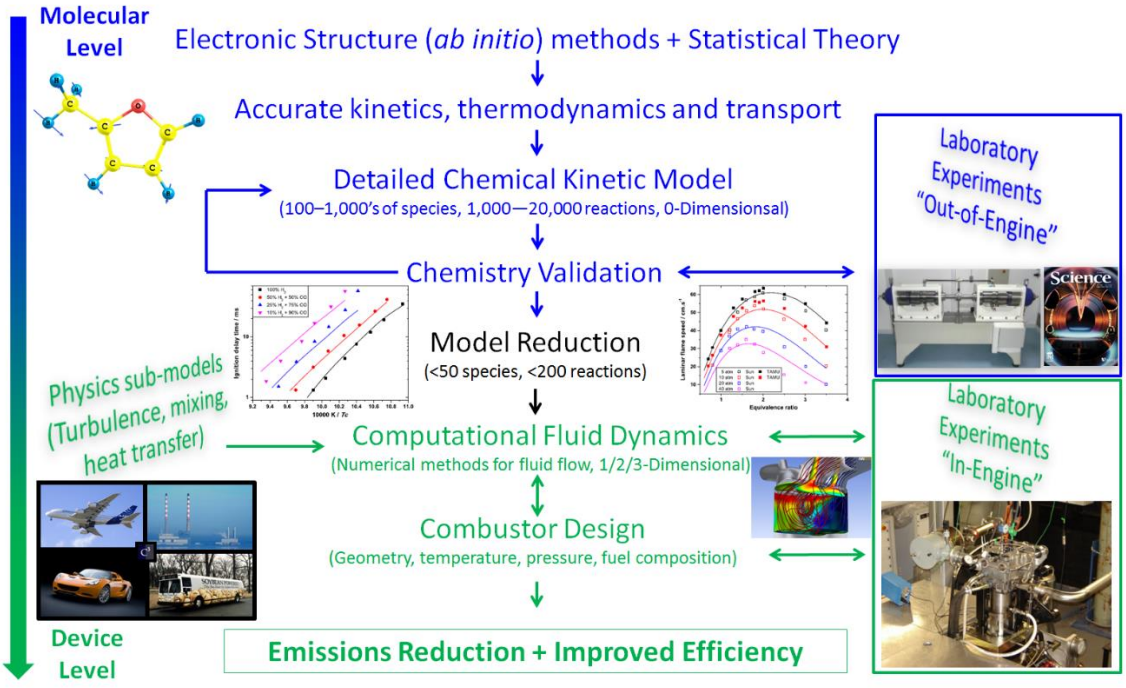

Fig. 1: Schematic diagram showing the steps in the development of the understanding of combustion and application to real devices.

There are broadly four levels of development that combustion researchers work in, (i) quantum mechanics and direct kinetic measurements of rate constants and reaction intermediate and products, (ii) fuel structure and fundamental chemistry, (iii) CFD studies with reduced chemistry and (iv) practical applications. Electronic structure, ab-initio methods and statistical theory lies at "level 1". These are used to calculate accurate thermochemical parameters and rate constants for the species involved in chemical reactions. At "level 2", these species and reactions are amalgamated into detailed chemical kinetic mechanisms which are validated by comparing to experimental measurements, starting with homogeneous reactors and laminar flames, and steadily getting more complex (rapid compression machines and engines) and more practical at level 2. At level 3 chemical kinetic mechanisms are reduced in the number of species and reactions, simultaneously retaining a target feature e.g. ignition delay time, flame speed, emissions predictions, etc., so that they can be used in combination with chemical reactor networks or computational fluid dynamic simulations in novel designs of cleaner, more efficient combustors. At level 4 are the practical applications people who study jet engines, diesel engines, natural gas safety, fuel inhibition, etc.

Very few individuals/groups work at all four levels. This paper will focus largely on level 2, the development of detailed chemical kinetic mechanisms which depend on fuel structure and fundamental kinetics. There will be some discussion and comment on level 1 where quantum chemistry plays an increasingly important role in the development of detailed kinetic models.

The chemical kinetic modelling community has had considerable success in developing reliable chemical kinetic mechanisms for fuel combustion. GRI-Mech [1]–[3] was one of the first mechanisms freely available on the internet developed to simulate natural gas mixtures and included NOx chemistry [3] to help with emissions predictions. The primary reference fuel (PRF) (*n*-heptane and *iso*-octane) mechanisms published from Lawrence Livermore National laboratory [4], [5] have also been very useful as they also are freely available on the internet and describe the two fuels that are/were used as surrogates for gasoline fuel and *n*-heptane for diesel fuel. Further work has been performed on developing mechanisms describing even larger hydrocarbon and oxygenated hydrocarbon molecules [6], [7] and surrogate mechanisms [8]. These have been followed by recent successes in the development of jet-fuel surrogates formulated using real fuel properties [9], [10] and discussed in more detail by Dryer [11]. Generally, predictions using published chemical kinetic mechanisms describing the pyrolysis and/or oxidation of a fuel are within less than a factor of two of experimental measurements. However, despite the many successes in the community over the years there remains a lot of potential improvements. The prediction of ignition delay times for any fuel at temperatures above 1100 K typically depends on the kinetics describing the underlying C_0–C_4 species. However, there is no commonly accepted community mechanism available to describe C_0–C_4 fuel oxidation over a wide range of temperature, pressure, equivalence ratio, and dilution. In addition, we do not have a go-to database for the thermodynamic parameters of species contained in chemical kinetic mechanisms. Similarly, databases containing libraries of measured validation data to develop reliable predictive mechanisms need to be developed.

1.1 What is a kinetic model?

A chemical kinetic mechanism contains species with associated thermodynamic and transport properties and elementary chemical reactions and associated rate constants. For instance, the oxidation of hydrogen can be described using the global reaction $H_2 + ½O_2 = H_2O$ and that for methane by $CH_4 + 2O_2 = CO_2 + 2H_2O$. However, these reactions do not occur as written. Hydrogen requires eight species and approximately 30 elementary reactions to describe its oxidation over a wide range of pressure and temperature. For methane the mechanism is even more complex—requiring approximately 30 species and 200 elementary reactions. An

elementary reaction specifies the reactant and product species and the associated rate constant. The forward rate of the elementary reaction A ⇌ B can be written as k_f[A] and that in the reverse direction k_r[B], where k_f and k_r are the forward and reverse rate constants, respectively. The expression for the rate constant can be written in the Arrhenius form [12] where $k = A \times \exp(-Ea/RT)$ or modified Arrhenius form [13], [14] where $k = A \times T^n \times \exp(-Ea/RT)$. At equilibrium the forward and reverse rates are equal, so we can write $K_p = k_f/k_r = [B]/[A]$ (in this case $K_p = K_C$ as $\Delta n = 0$). In the Arrhenius form, knowing that $K_p = \exp(-\Delta G_r/RT)$ it can be shown that $A_f/A_r = \Delta S_r/R$ and $\Delta H_r = E_f - E_r$. Thus, from a knowledge of the forward rate constant and the thermochemical parameters of the reacting species it is possible to calculate the reverse rate constant and allow for thermodynamic equilibrium. A kinetic model contains a listing of both the species with their thermodynamic parameters and all of the elementary reactions and their associated rate constants and third body collision efficiencies. For problems involving diffusion, transport properties are also required.

In order to use a chemical kinetic model, a numerical model is required to simulate practical devices, such as shock tubes, rapid compression machines, flow- and jet-stirred reactors, burner-stabilized flames, etc. Programs that are commonly used in simulating chemically reacting systems include Reaction Design's CHEMKIN suite [15], OPENSMOKE [16], [17], Cantera [18], [19], LOGESoft [20], FlameMaster [21], CMCL Innovations' *k*inetics [22], DETCHEM [23], Cosilab [24] and Workbench [25]. These numerical models solve a series of differential equations that require initial conditions from the experiments to be simulated. For example, for a shock tube, these initial conditions include the fuel/O_2/diluent composition and the gas temperature and pressure. Thereafter, a system of differential equations consisting of the species and energy conservation equations must be solved. The integration of these equations proceeds in timesteps using integration control to ensure that the species, temperature and pressure do not change considerably in any one timestep so that the overall calculation is accurate. When a shock tube ignition is computed, initially the only reactions that are important are the unimolecular fuel decomposition reactions and the reaction of the fuel with molecular oxygen. As reaction progresses in time, higher concentrations of smaller radical species are produced, eventually leading to autoignition of the fuel. For multi-dimensional experiments, e.g. burner-stabilized flames, diffusion and transport of species is important and contributes to the species and energy conservation equations, so that the transport properties of all of the species must be included in the calculation. Thus, transport properties for all of these species are needed and this highlights the need for accurate transport properties. There has been a recent study by Liu et al. [26] discussing the theory and experiment of binary diffusion coefficients of *n*-alkanes in diluent gases, who refer to previous work by Violi and co-workers [27], [28], Jasper et al. [29] and Jasper and Miller [30] on the subject. Typically, the most important species controlling the reactivity in flames are hydrogen atoms as these are light and can diffuse easily from the reaction zone into the unburned gases of a flame. The importance of Ḣ atoms in flames is demonstrated by sensitivity analyses which show high sensitivity to reactions producing and consuming them.

The process involved in developing chemical kinetic models has been described previously by Miller, Kee and Westbrook [31] Frenklach et al. [32] and Simmie [33]. Typically, models are validated by simulating a wide range of experimental targets, including ignition delay times, flame speeds and species concentration measurements in flow- and jet-stirred reactors and in flames. A well-validated oxidation model is one which can simulate a fuel's oxidation over a wide range of physical conditions including mixture compositions, temperatures and pressures. What determines whether a mechanism can do so or not is whether or not all of the relevant reaction pathways are included in the mechanism and whether the values/accuracy of the rate constants used are sufficiently accurate. It is the aim of a chemical kinetic modeler to determine the thermodynamic, rate constant and transport parameters (*A, n, Ea* and ΔG) for

each species/reaction with "chemical accuracy" ensuring that all relevant reaction pathways and/or reaction product channels are included. This is achieved either by experiment or theoretically-and is non-trivial for the ranges of temperature/pressure/fuels encountered in the laboratory and/or in practical devices.

1.2 A brief history of chemical kinetic modeling

Advances in chemical kinetic modelling in terms of the size of the molecules and number of reactions that can be treated have largely paralleled the increase in computer capabilities. Westbrook et al. [34] in their 2004 review of computational combustion point to Moore's law [35] which predicts a doubling of computing power every 18–24 months and this allowed the development of ever larger chemical kinetic models. This was well illustrated in the review by Lu and Law [36] and is presented here again in Fig. 2, which shows a comparison of advances in computing capability with time, Fig. 2(a) and the size of chemical kinetic models, Fig. 2(b) which is taken from the work by Egolfopoulos et al. [37].

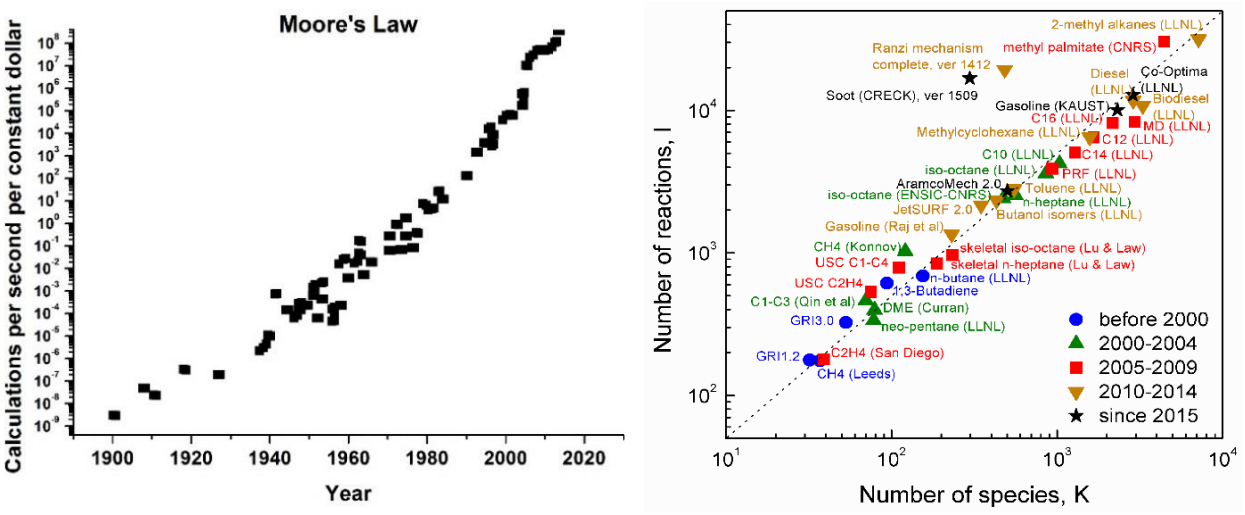

Fig. 2: Illustration of the correlation between computer power and mechanism size.

Westbrook et al. [34] describe the early development of chemical kinetic mechanisms, all facilitated by the development of stiff kinetic equation solvers [38], [39] with the first chemical systems to be modeled being those describing ozone [40] in 1953 and hydrazine decomposition [41] in 1956, followed by models describing hydrogen combustion followed by methane [42]–[46] and methanol [47], [48], in the late 60's and 70's. Shortly thereafter Westbrook and Dryer [49], [50] presented the concept of the hierarchical nature of mechanism development in which mechanisms for larger hydrocarbon species include those for the underlying hydrogen/oxygen, and hydrocarbon and oxygenated hydrocarbon species. Furthermore, the mechanism for methane was shown by Warnatz [51], [52] to be complicated by the recombination of methyl radicals to produce ethane, with further consumption producing ethylene and acetylene and resulted in one of the first presentations of a flux diagram, similar to Fig. 3. Note that, based on this diagram, it requires approximately 30 species to describe the oxidation of methane. However, it requires many more, including the addition of poly-aromatic species, if the study involves pyrolysis conditions.

It is worth noting that in simulating ethane oxidation under fuel-rich conditions, it is necessary to include the mechanisms describing propane (produced by the recombination of $\dot{C}H_3$ and $\dot{C}_2H_5$ radicals) and butane (produced by the recombination of two $\dot{C}_2H_5$ radicals) oxidation to

accurately simulate experimental targets. Many other detailed chemical kinetic mechanisms describing methane/ethane kinetics have been developed over the years including those for natural gas from Dagaut and co-workers [53]–[55], a methane/ethane mechanism from Barbé et al. [56], the Leeds methane mechanism [57], the Miller-Bowman NO mechanism [58], and those for small oxygenated species from the Dryer group [59]–[62]. Moreover, Frenklach et al. [31], [63] recommended the development of optimal reaction mechanisms by fitting rate constant parameters to a wide range of experimental data targets. This culminated in the generation of various iterations of GRI-Mech [1]–[3] which is an optimized mechanism, designed to provide sound basic kinetics. At the time of their publication, these mechanisms furnished the best combined modeling predictability of basic combustion properties used to simulate natural gas combustion, including NO formation and re-burn chemistry.

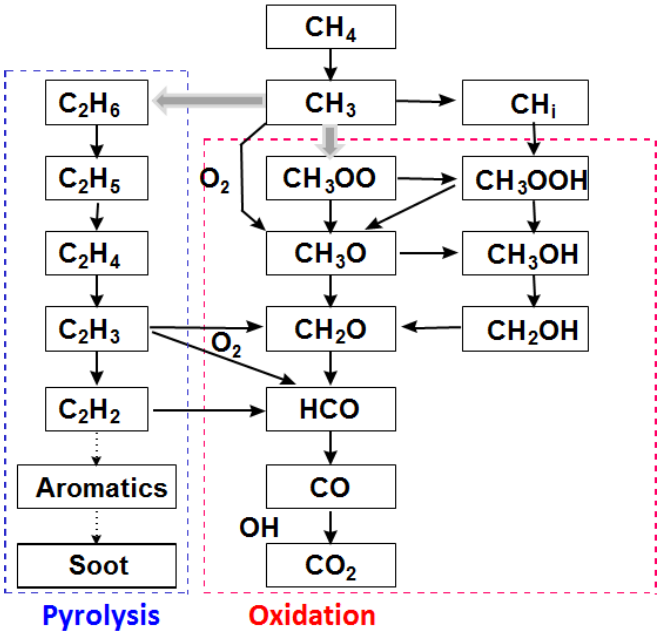

Fig. 3: Mechanism for $\dot{C}H_3$ and $\dot{C}_2H_5$ oxidation (courtesy of Prof. Eliseo Ranzi) as originally described by Warnatz [51].

An extensive range of targets were chosen for GRI-Mech including (i) shock tube ignition delay times for pure methane and ethane fuels in addition to methane/ethane and methane/propane mixtures, (ii) methane and ethane shock tube species profiles, (iii) H_2/CO, methane and ethane flame speed measurements. Moreover, some acetaldehyde and vinoxy chemistry are included to better describe ethylene oxidation, and because natural gas contains propane, a minimal set of propane kinetics is included to model this (and other larger) species. GRI-Mech 3.0 also includes as targets shock tube observations sensitive to the oxidation of the formaldehyde intermediate; a set of shock tube, low pressure flame, and flow reactor experiments concerning prompt NO formation and reburn; and some targets concerning the shortening of methane shock tube ignition delays by small amounts of propane or ethane.

One of the great successes of GRI-Mech was not only in the comprehensive range of its validated applicability, but the fact that it was among the first to be made freely available on the internet. Furthermore, it tends not to run into problems of stiffness experienced by many other kinetic mechanisms.

More recently, Williams et al. developed versions of San Diego Mech [64], [65] and Wang et al. have developed USC Mech II [66] and JetSurf [67] in addition to the CRECK mechanism from the Politecnico di Milano [68], [69], AramcoMech [70]–[72] from NUI Galway and Glarborg Mech [73] which all present detailed mechanisms to simulate the oxidation of small

hydrocarbons systems with the mechanisms freely available on the internet. All of these mechanisms have evolved from somewhat different, but very similar, versions of the same mechanism involving similar reactions but with different rate constants. Some of these mechanisms were developed to be used as community-wide core C_0–C_4 mechanisms e.g. San Diego Mech, USC Mech II, JetSurf and AramcoMech while other groups rely on in-house core mechanisms e.g. the CRECK mechanism.

As stated earlier these mechanisms form the basis of all larger hydrocarbon mechanisms (see Fig. 4). It is now commonly accepted that it is possible to (automatically) generate mechanisms by first generating a core C_0–C_4 mechanism and then building larger components upon this. In addition, because these molecules are relatively small (and volatile), there have been a lot of experimental and theoretical studies of the rate constants in the range of C_0–C_4 with each elementary reaction being treated individually. Extensive validation experiments usually exist and many of the elementary reactions are rather idiosyncratic or unusual with the principal reactions being $\dot{H} + O_2 = \ddot{O} + \dot{O}H$ and $CO + \dot{O}H = CO_2 + \dot{H}$. Thus, current state-of-the-art mechanisms describing C_0–C_4 kinetics include rate constants that have mostly either been measured or calculated from quantum chemistry which are becoming more and more accurate and have greatly improved the predictive capability of chemical kinetic mechanisms.

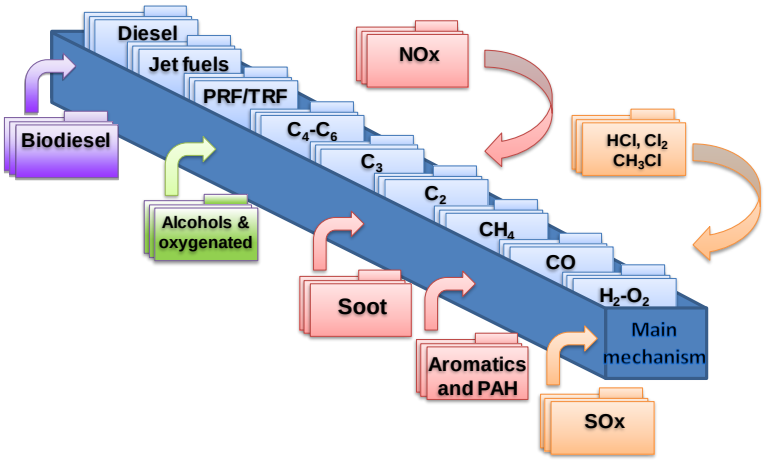

Fig. 4: Schematic (courtesy of Prof. Eliseo Ranzi) showing component library for detailed mechanism development.

In the past, species and reactions were reviewed and evaluated by Cohen and Westberg [74], [75], Tsang and Hampson [76]–[80], and with probably the most famous reviews by Baulch et al. [81]–[83] where rate constants were recommended. Furthermore, the NIST Chemical Kinetics Database is also available on the internet [84] but does not include recommendations and evaluations of rate constants. These reviews were performed reaction-by-reaction, examining every experimental study of each reaction that had been carried out. However, as indicated previously [70] such reviews have never addressed the combined effects of all of the reactions and species involved in these small-molecule models and, combining the recommended rate constants for each of the reactions in a chemical kinetic mechanism, would probably result in a mechanism incapable of predicting a wide range of experimental targets, if any target at all. In practice, a mechanism's performance is generally compared to experimental data and typically some optimization is required.

Typically, chemical kinetic modelers tend to adopt the best measured and/or calculated rate constant for important reactions in the literature and typically adjust the rate constants to fit a wide range of experimental targets including ignition delay times, flame speeds, species profiles measured as a function of temperature and/or time in flow and jet-stirred reactors or versus height above the burner surface in burner stabilized flames.

Sensitivity analyses of reaction rate constants to any of the target predictions mentioned above at high temperatures (> 1250 K) for non-aromatic species show that sensitivity is primarily due to the smaller species (C_0–C_4) chemistry. Fig. 5(a) shows sensitivity of changes in reaction rate coefficients to ignition delay times at 1300 and 1600 K. Sensitivity is observed for H_2/O_2 and C_1/C_2 species chemistry in addition to fuel decomposition reactions and fuel reactions with smaller radicals, which lead quickly to the generation of small (C_0–C_4) radical and olefinic species. In general, increasing the rate constants for fuel decomposition reactions and/or fuel + small radical species increases the rate of reaction, except for the reaction of the fuel with hydrogen atoms; this reaction normally reduces reactivity as it competes with the most important high-temperature chain-branching reaction $\dot{H} + O_2 = \ddot{O} + \dot{O}H$).

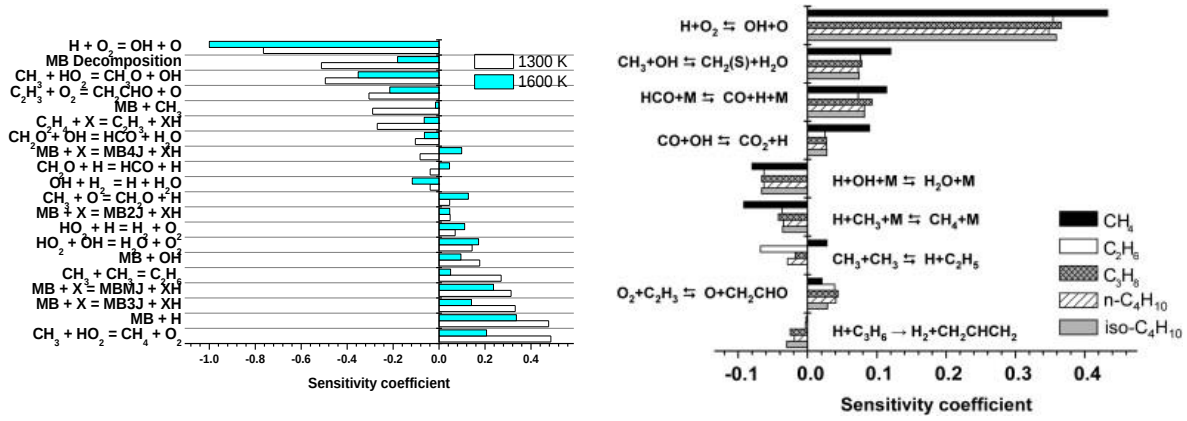

Fig. 5. Sensitivity coefficients at 1 atm to (a) predicted ignition delay time measurements resulting from factor of two changes in A-factor for reactions pertaining to 1.0% methyl butanoate oxidation, at $\varphi = 1$ in Ar [85] (b) laminar flame speed predictions, for small alkanes/air flames at $\varphi = 1$, $T = 298$ K. Reporduced from [68] with permission from Elsevier.

For flame speed predictions sensitivity is usually observed for reactions involving only H_2/O_2 and C_1/C_2 species chemistry with some sensitivity also due to allyl radical chemistry Fig. 5(b). Interestingly, flame speed predictions are not usually found to be sensitive to reactions pertaining to the parent fuel and thus including only the high temperature portion of a mechanism to reduce computational time is justified in their simulation. We will see later that, for non-aromatic fuel oxidation at low-temperatures (and for aromatic species at all temperatures), the parent fuel molecule reactions dominate and control reaction kinetics.

2. The H_2/O_2 system

Given the importance of the core C_0–C_4 chemistry it is understandable that so much effort has been dedicated to the generation of chemical kinetic mechanisms to accurately describe the underlying chemistry. The H_2/O_2 system is fundamental to all chemical kinetic mechanisms and recent chemical kinetic models describing this chemistry include similar reactions but with somewhat different rate coefficients. For the H_2/O_2 system the determination of rate parameters is usually based on direct kinetic measurements, and if not available are calculated using quantum chemistry.

Hydrogen oxidation is controlled by the competition between chain-branching and the pressure-dependent chain-propagation reactions:

$$\dot{H} + O_2 = \ddot{O} + \dot{O}H$$

$$\dot{H} + O_2 (+M) = H\dot{O}_2 (+M)$$

which controls and exactly reproduces the second limit of the hydrogen explosion diagram [86], Fig. 6(a). At a constant temperature of 800 K and at low pressures (< ~160 Pa) the first explosion limit is controlled by the rate of Ḣ atom diffusion to the walls of the reactor; if the rate of diffusion s fast enough to dominate over the rate of reaction with molecular oxygen then no explosion occurs. At pressures in the range of ~160 – 5000 Pa the rate of the chain-branching reaction Ḣ + O_2 = Ö + ȮH is fast, and explosion occurs. Above ~5000 Pa (~0.05 bar) the rate of the reaction Ḣ + O_2 (+M) = $HȮ_2$ (+M) becomes competitive with the chain-branching reaction and no explosion is occurs. The 3rd explosion limit is reached at a pressure of ~500 kPa (~5 bar). Liang and Law [87] have recently shown that this is controlled by a competition between the gas-phase chemistry of $HȮ_2$ radicals and H_2O_2 molecules competing with reactor wall deactivation; $HȮ_2$ radical becomes essential at the turning point from the second to the third limit in the intermediate pressure range, and H_2O_2 is the controlling species at the high pressures of the third limit.

The resulting variation in predicted ignition delay times as a function of pressure and temperature is illustrated in Fig. 6(b), which is taken from the work of Kéromnès et al. [88], and is discussed there.

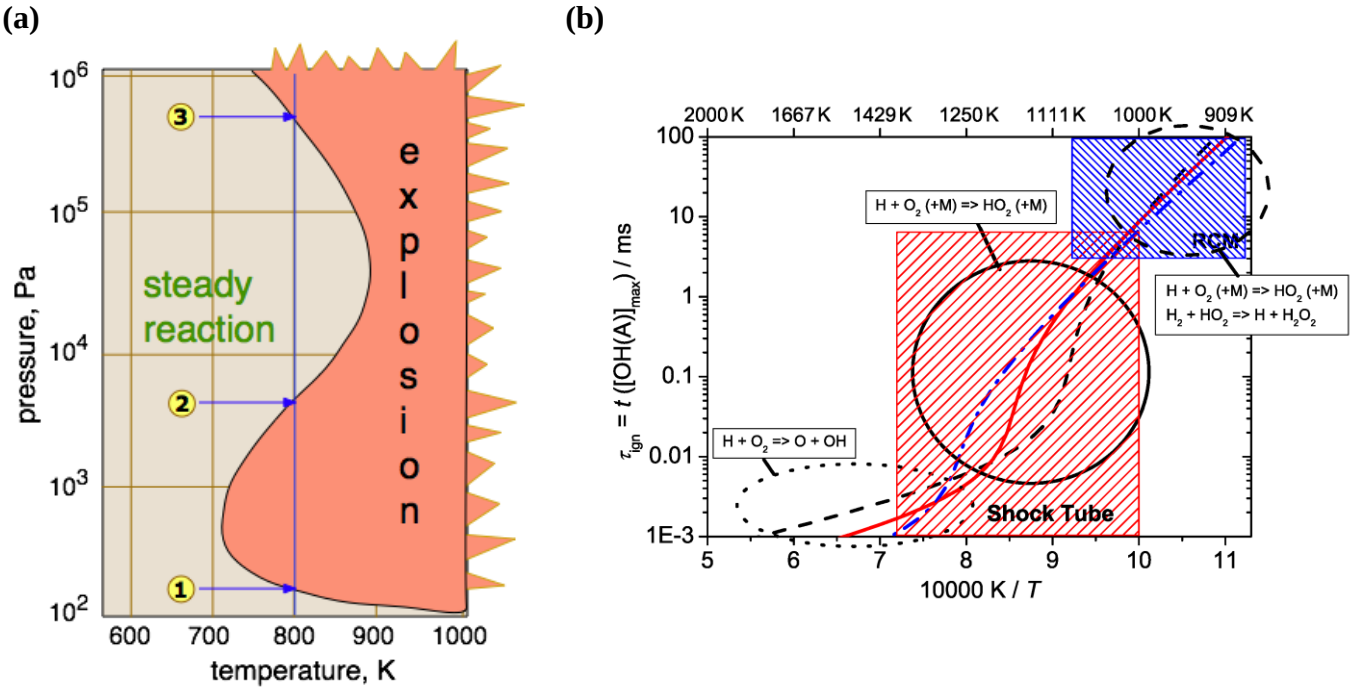

Fig. 6: (a) Explosion limits of hydrogen/oxygen mixtures as a function of pressure and temperature. (b) Main reactions and ignition delay times as a function of temperature for a mixture of 0.7 H_2 + O_2 + 3.76 Ar tested using the Li et al. [89] mechanism at 8 bar (- - -), 16 bar (—) and 32 bar (- ⋆ -). Figure 6(b) reproduced from [88] with permission from Elsevier.

2.1 Optimizing the H_2/O_2 system

By updating the Li et al. [89] mechanism to describe the H_2/O_2 system Burke et al. [90] primarily relied on fundamental measurements of rate constants to interpret and simulate experimental data. Ab initio calculations were used to calculate rate constants for important reactions in the H_2/O_2 system and modeling studies indicated that the reaction Ḣ + $HȮ_2$ = H_2O + Ö should be included in the mechanism. A detailed interpretation of experimental data also suggested that ignition delay time measurements in shock tubes are sensitive to potential impurity effects, which accelerate early radical pool growth in shock tube speciation studies. In

addition, speciation predictions in burner-stabilized flames were more sensitive to uncertainties in experimental boundary conditions than to uncertainties in kinetics and transport.

Kéromnès et al. [88] developed a mechanism to describe syngas oxidation using rate constants from the literature and, by performing sensitivity analyses, adjusted the rates of the reactions $\dot{H} + O_2 (+M) = H\dot{O}_2 (+M)$, $H_2O_2 (+M) = \dot{O}H + \dot{O}H (+M)$ and $H_2 + H\dot{O}_2 = H_2O_2 + \dot{H}$ within their uncertainty limits primarily based on ignition delay time measurements in a rapid compression machine at low temperatures and high pressures.

Hashemi et al. [91] updated the Burke et al. mechanism by adjusting the rate constants, based on recent determinations for the literature, for the reactions $H\dot{O}_2 + \dot{O}H$ [92], $\dot{O}H + \dot{O}H$ [93], and $H\dot{O}_2 + H\dot{O}_2$ [94] and their own flow reactor measurements of species profiles versus temperature. These studies performed by Kéromnès et al. [88] and Hashemi et al. [91] and to a lesser extent by Burke et al. [90] involved the development of a chemical kinetic mechanism "by hand" by optimizing rate parameters using both direct and indirect measurements.

Most recently, Turányi et al. optimized the rate constants in a H_2/O_2 mechanism [95] with a mathematical technique employing both direct (absolute value measured directly) and indirect (rate constant derived by fitting to measured ignition delay times, intermediate species profiles, flame speed, etc.) measurements [96]. This type of optimization was first proposed by Frenklach and Miller [97]–[99] who described an algorithm [31] that was used in the generation of the GRI mechanisms [1]–[3]. Frenklach et al. further developed the mechanism optimization approach towards data collaboration [100]–[104], which is a method that unites process models and associated admissible parameter values with experimental data and accompanying uncertainties, and provided an implementation of the method on the PrIMe (**Pr**ocess **I**nformatics **M**od**e**l) website [105]. It involves starting with an initial mechanism which is parameterized on the basis of data evaluations. Thereafter, indirect measurement data (called "optimization targets") are selected. These data included ignition delay times, flame speeds, and species concentration measurements in flames and in flow- and jet-stirred reactors. Using local sensitivity analysis, the important reactions at the experimental conditions are identified. The frequency (*A*)-factors of the important reactions (and certain enthalpies of formation and third-body efficiencies) are referred to active parameters. The uncertainty limits of the *A*-factors are determined on the basis of the *f* uncertainty parameters of the data evaluations, and the active parameters are optimized within the uncertainty limits to achieve the best agreement with the targets and are thus based on the direct measurements. This method was also employed by Wang et al. [106]–[108]. A recurring problem of this method lies in that the optimized *A*-factors tend to move to the extremes of their uncertainty limits. To overcome this Frenklach et al. [109] and Sheen and Wang [110] extended the objective function such that a deviation from the evaluated *A*-factor (evaluated based on direct measurements) was also penalized and resulted in the optimized *A*-factors being closer to the recommended rate constants.

Scire et al. [111] proposed a method for the derivation of the rate coefficients by fitting parameters of a complex reaction mechanism to species profiles measured for moist CO oxidation perturbed with methane in a high-pressure flow reactor. They suggested importance-sampled Monte Carlo calculations, in which the parameter values were distributed according to their uncertainties. The method provided not only optimized rate coefficients but also rigorous error estimates.

The work of Turányi et al. [96] is similar to that of Frenklach and Wang with several differences. Firstly, the experimental results related to rate coefficient determinations are considered directly and not via an evaluated value based on the direct measurements. Secondly, the original indirect measurement data are used instead of a "target value" deduced from a

series of indirect measurements at given conditions. Thirdly, the uncertainty domain of all Arrhenius parameters (*A*, *n* and *Ea*) are determined and not only the uncertainty limits of the *A*-factors. Finally, all Arrhenius parameters and other influential rate parameters (low-pressure limit, M = N_2) and third-body efficiency values are optimized and not just the *A*-factors. This is important as optimizing only *A*-factors will result in a mechanism that cannot be used over a wide range of temperature and/or pressure. This method has been successfully applied by Turányi's group in developing optimized mechanisms describing H_2/syngas [95], methanol and formaldehyde [112] and ethanol [113]. In these studies rate constants for the important reactions are presented with their prior and posterior uncertainty ranges by plotting available literature rate constant data, either measured, calculated or derived from fitting to a complex mechanism. This type of optimization is superior to those by Frenklach and Wang as the derived rate constants are fit over a wide range of temperature (and pressure) and thus leads to a more widely applicable chemical kinetic mechanism. Using all targets too does not include a prior prejudice to experimental data but posterior analysis can lead to the identification of outliers which the optimized mechanism struggles to simulate.

Recently, Bernardi et al. [114] developed a generalized framework called Curve Matching (CM) for the comparison of models with experiments, using *n*-heptane as an example. The approach relies on the transformation of discrete experimental data and the relative numerical predictions to two different continuous functions. In this way, CM allows not only the comparison of errors, similar to the work of Turányi et al. [115], [116] (i.e. the differences between the experimental and calculated values), but also the shapes of the measured and numerical curves (i.e. their first derivatives) and possible shifts along the *x*-axis (e.g. temperature, inverse temperature or time). These features permit the limitations of the Sum of Squared Error based methods, which do not account for the shape of curves, to be overcome.

The approaches to chemical kinetic modeling discussed above use constraints imposed by combustion targets on combinations of rate parameters (and vice versa), with their reliability limited to systems where (i) sufficient data is available to constrain the rate constants over the full range of physical conditions of temperature/pressure/mixture composition of interest and (ii) full uncertainties in the temperature/pressure/mixture composition dependence of rate constants are considered. Recently, Burke et al. [117], [118] have promoted a multi-scale modeling approach by using theoretical kinetics calculations in combustion model development directly, replacing the dependence on rate constant fitting expressions with a physically meaningful kinetic theory. The theoretically calculated rate constant expressions can be first verified by comparison with experimental measurements, and because they are based on proven theory can be extrapolated beyond the range of physical conditions for which data currently exist. This approach is laudable but considering that detailed chemical kinetic mechanisms, even describing propane oxidation, can contain many hundreds of elementary reactions it has historically been intractable to calculate at a high-enough level of theory for all of the important rate constants. There have been some advances in the community to develop software to help automate calculations of potential energy surfaces. Zádor and Najm [119] have developed an automated code, KinBot, to explore reaction pathways in the gas phase and was used successfully by Zádor and Miller [120] in mapping the $C_3H_5\dot{O}$ PES. The quantum chemistry methods employed need to be of high enough level to provide appropriate accuracy of these important pathways. In the future, it is probable that other codes, similar to KinBot, will be developed for automatic mechanism generation directly from quantum chemistry. This concept has been advanced further by Keceli et al. [121] who describe the development of codes to automatically generate high-fidelity mechanisms through exascale-level predictive automated combustion kinetics (PACK) calculations. This effort combines mechanism generation, theory-based calculations of rate constants, thermochemistry and transport properties, in addition to mechanism reduction, all designed to be implemented automatically.

Discussed above are methods used for mathematical optimization and optimization based on "non-mathematical methods" and/or "expert/tacit knowledge". Most groups optimize their mechanisms manually, and there is as much value to doing this as there is to the Turányi/GRI approach. One point to note with the approach is that the more direct and indirect measurements available for a given fuel the more successful the optimization will be. The relative success of GRI-Mech at the time and the recent successes by Turányi et al. [93], [112] may be limited due to the lack of extensive validation data available for larger species. In these systems, “expert knowledge” will have an advantage.

Chemical kinetic modelers who optimize by hand tend to have a tacit and tangible knowledge of the reaction pathways of the fuel and intermediate products. While automatic optimization has advantages if there is a clear approach to doing so, it does not require, and may not result in, the intrinsic knowledge gained in doing things by hand. There is no clear-cut method to optimize a mechanism. It can also be argued that one should not optimize a mechanism at all, but rather allow the mechanism make predictions based on the high-level quantum chemistry calculations and/or measurements of the rate constants it contains. This will then inform one as to whether further species/reactions are missing or whether a higher level of theory/understanding needs to be applied. Moreover, it may be argued that optimization may lead to incorrect rate constant choices if important reaction pathways are missing from a mechanism. These arguments have their merits but if models are needed to make “accurate” predictions of chemical behavior for practical problems, then some level of optimization, within the uncertainties of the rate constants, is warranted given the current state-of-the-art.

3. Kinetic databases for model validation

One of the most important components in developing chemical kinetic models is having reliable data with which to validate the model. In the past groups have compiled these data over time, either by digitally extracting the data from figures in journal articles or by contacting the authors of papers and generating in-house libraries. If these are not maintained over time, then the data can be lost. Moreover, the original source may not be accessible as the principal investigator may have retired and/or the researcher who took the data may have left the group with the result that it can no longer be located. Furthermore, there can be some discussion as to what data is needed to be recorded. To simulate ignition delay times for example, the initial fuel/oxidizer/diluent concentrations are needed as input to the simulation in addition to the reflected shock temperature and pressure. However, frequently the experimental pressure/time histories of each experiment would be useful information to have to test for facility effects, particularly pre-ignition pressure rise. To this end, Frenklach et al. developed the PrIMe website [102]–[105] which unites process models and associated admissible parameter values with experimental data and accompanying uncertainties with one of its primary goals being the collection and storage of data, validating the data and qualifying uncertainties. Recently, a new database called ReSpecTh [122], [123], has been created for the distribution of data files, programs, and results related to mechanism development and optimization. The ReSpecTh Kinetic Data format (RKD format) is a slightly modified form of the PrIMe data format, containing files of the indirect and direct experimental data to be processed. Currently, data have been entered for testing and optimizing hydrogen, syngas, methanol and ethanol combustion mechanisms. Weber and Niemeyer [124] have also developed a human- and machine-readable data standard, ChemKED, for storing fundamental experimental data.

4. Distinct temperature regimes for autoignition chemistry

Figure 7 shows model simulated ignition delay times for *n*-pentane oxidation in 'air' at 20 atm using the mechanism by Bugler et al. [125]. Three equivalence ratios are simulated, varying from fuel-lean (φ = 0.5) through stoichiometric (φ = 1.0) to fuel-rich (φ = 2.0). Three distinct temperature ranges of reactivity can be observed, low (600~750 K), intermediate (900~1250 K), both included in the negative temperature coefficient (NTC) regime, and high temperatures (> 1300 K).

At low temperatures the chemistry is more complex where chain branching stems from the addition of fuel radicals to molecular oxygen in the sequence of reactions: $\dot{R} + O_2 \rightarrow R\dot{O}_2 \rightarrow \dot{Q}OOH + O_2 \rightarrow \dot{O}_2QOOH \rightarrow R\dot{O} + \dot{O}H + \dot{O}H$. This sequence depends on the fuel radical concentration and we observe that fuel-rich mixtures are fastest to ignite, whereas fuel-lean mixtures are slowest in this temperature regime [126]. Evidence supporting this understanding was published in 2011 by Yamamoto et al. [127] who reported stabilized three-stage oxidation of gaseous *n*-heptane/air mixtures in a micro flow reactor. Discussions on reactions important at intermediate temperatures have been provided previously, e.g. Westbrook [128] in his invited topical review, but these generally do not include the importance of the concerted elimination reaction ($\dot{R}O_2$ = olefin + $H\dot{O}_2$) in this regime.

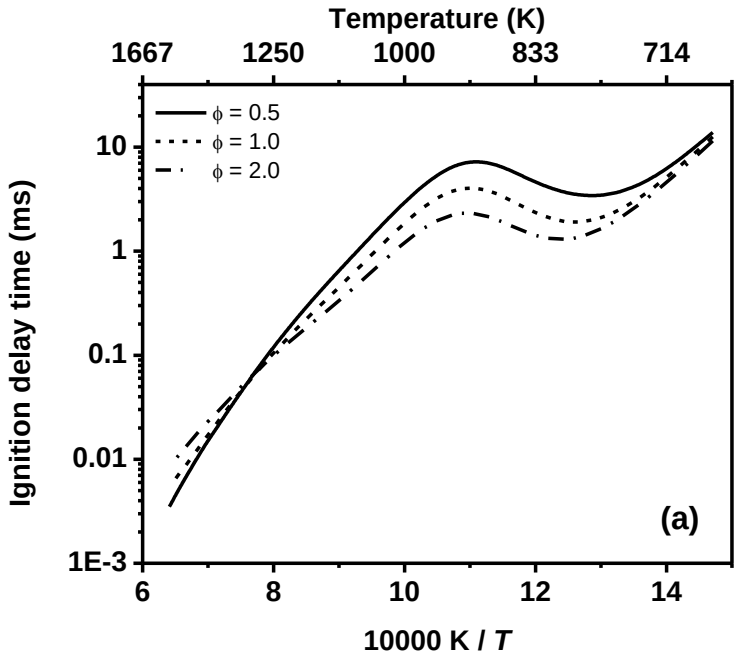

Fig. 7: Model predicted ignition delay times for *n*-pentane oxidation in 'air' at 20 atm using the mechanism developed by Bugler et al. [125].

At intermediate temperatures (~950–1300 K) chain branching is controlled by the sequence of reactions:

$$\dot{H} + O_2 (+M) = H\dot{O}_2 (+M)$$
$$RH + H\dot{O}_2 = \dot{R} + H_2O_2$$
$$H_2O_2 (+M) = \dot{O}H + \dot{O}H (+M)$$
$$\dot{R} + O_2 \rightleftharpoons \dot{R}O_2$$
$$\dot{R}O_2 = \text{olefin} + H\dot{O}_2$$

The reactions of fuel with hydroperoxyl radicals and the molecular elimination reactions of alkyl-peroxyl ($\dot{R}O_2$) radicals forming an alkene and a hydroperoxyl radical all depend on fuel concentration. The higher the concentration of the fuel, the faster the rate of oxidation.

At approximately 1300 K, the ignition delay times at all three equivalence ratios are the same, where the underlying chemistry is transitioning from being dominated by low- to intermediate-temperature chemistry to high temperature kinetics. At temperatures above 1300 K, experimental shock tube data and model predictions show that fuel-lean mixtures are fastest to ignite whereas fuel-rich mixtures are slowest. At high temperatures the main chain-branching reaction controlling the chemical rate stems from the following sequence of reactions:

$$\dot{H} + O_2 = \ddot{O} + \dot{O}H$$
$$\ddot{O} + H_2 = \dot{H} + \dot{O}H$$
$$\underline{\dot{O}H + H_2 = H_2O + \dot{H}}$$
$$\text{Net: } 2H_2 + O_2 = \dot{O}H + \dot{H} + H_2O$$

At these temperatures the rate constant for $\dot{H} + O_2 = \ddot{O} + \dot{O}H$ becomes faster than that for $\dot{H} + O_2 (+M) = H\dot{O}_2 (+M)$ and thus dominates at these temperatures. In addition, fuel-lean mixtures contain relatively higher concentrations of molecular oxygen and thus the rate of the reaction will be in proportion to its concentration.

4.1 Developing a core high-temperature mechanism

Since the oxidation of any fuel at high temperatures depends largely on C_0–C_4 chemistry, the development of accurate and comprehensively validated mechanisms describing the oxidation of small molecule core species is extremely important. As mentioned earlier mechanisms describing the oxidation of small hydrocarbon species have been published [64]–[73] which include detailed mechanisms to simulate the oxidation of methane, ethane, ethylene, acetylene, formaldehyde, acetaldehyde, methanol, and ethanol in addition to the C_3 species including propane, allene and propyne. These have met with considerable success. These are the mechanisms that are generally used throughout the community because, as depicted in Fig. 5, the chemistry contained in them largely controls the high-temperature reactivity of all hydrocarbon and oxygenated hydrocarbon fuels. A good review of the important reactions pertaining to the associated sub-mechanisms of the species is given in the work by Metcalfe et al. [70]. In methane oxidation, for example, the rates of the reactions $H\dot{C}O + M = \dot{H} + CO + M$ and $H\dot{C}O + O_2 = CO + H\dot{O}_2$ and particularly their branching ratios are important in predicting flame speeds, with the former reaction producing $\dot{H}$ atoms and thus enhancing reactivity while the latter competes with it, producing $H\dot{O}_2$ radicals (rather than $\dot{H}$ atoms) and thus inhibits reactivity. The reaction $\dot{C}H_3 + \dot{H} (+M) = CH_4 (+M)$ is also very important in the prediction of flame speeds and ignition delay times at high temperatures. The rate constants used for this reaction vary among the different mechanisms with high-level quantum chemistry calculations available from Harding and Klippenstein et al.[129], [130] and usually include a high-pressure limit [130], a low-pressure limit and Troe parameters [131] so that the reaction can include pressure fall-off effects. One important feature of this reaction in flames is the effect of third-body colliders on the rate of reaction.

Fig. 8 shows flame speeds measured for methane oxidation at 1, 5, 10 atm, in which the burning velocity of methane decreases with increasing pressure due to the increased free-stream density and the influence of pressure-dependent radical chain termination reactions. One such reaction is the recombination of $\dot{H}$ atom with methyl radicals, which increases with pressure, and thus contributes to a reduction in the reactivity of the system. Fig. 8 shows that GRI-Mech 3.0 [3] captures the 1 atm data quite well, but is slower compared to experiment at the higher pressures of 5 and 10 atm. In GRI-Mech 3.0 the reaction is written in the Troe

format [131] with the rate constant enhanced by H_2 × 2.0, H_2O × 6.0, CH_4 × 3.0, CO × 1.5, CO_2 × 2.0, C_2H_6 × 3.0 and Ar × 0.7. By artificially setting all of these enhancements to 1.0 in GRI-Mech 3.0 the model is closer to the reported experimental measurements at 5 and 10 atm but becomes faster than the experimental data at 1.0 atm, as indicated by the dotted lines in Fig. 8. Several experiments and recent theoretical investigations (e.g., [132]) have been performed to gain insights into the process of energy transfer, but significant uncertainties remain, particularly in the case of water.

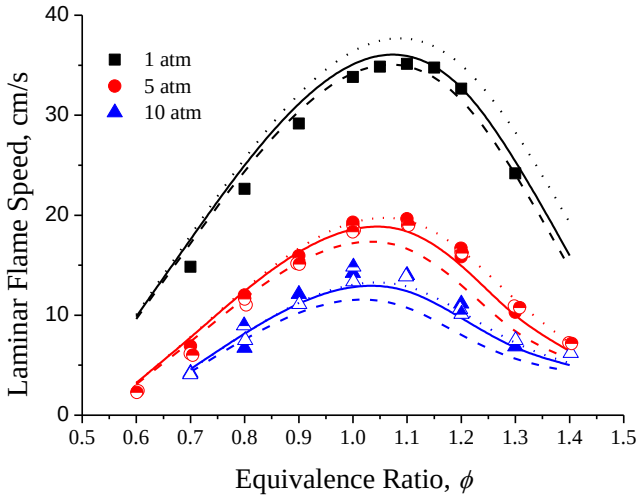

Fig. 8: Effect of third-body collider efficiency on CH_4 flame speed predictions in air at 298 K. Symbols are experimental data: Solid: Lowry et al. [133], semi-solid Gu et al. [134], open: Rozenchan et al. [135]. Lines are mechanism predictions: solid: AramcoMech 1.3 [70], dashed: GRI-Mech 3.0 [3], dotted GRI-Mech 3.0 with all colliders set to 1.0. Reproduced from [70] with permission from John Wiley and sons.

Third-body efficiency effects may also be important for oxy-fuel combustion in which fuel is burned in the presence of pure oxygen rather than air, thus producing high concentrations of carbon dioxide and water. Under these conditions the rate of reactions is likely enhanced by the collision efficiencies of H_2O, CO_2 and CO, particularly for the reaction $\dot{H} + O_2 (+M) = H\dot{O}_2 (+M)$ which competes with the main high-temperature chain-branching reaction $\dot{H} + O_2 = \ddot{O} + \dot{O}H$.

A mentioned above, to account for the pressure-dependent effects associated with rate constants, Troe [131] introduced a broaden factor, *F*, to fit the pressure fall-off rate constant,

$$\frac{k_u}{k_\infty} = \frac{k_0/k_\infty}{1 + k_0/k_\infty} F(k_0/k_\infty),$$

$$\log F\ (k_0/k_\infty)\ \approx\ \frac{log\ F_{cent}}{1 + (log k_0/k_\infty)^2}$$

This fit can sometimes lead to un-necessary inaccuracies. Recently, a generalized polynomial (PLOG) fit, of the temperature- and pressure-dependent polynomials was proposed by James Miller [136]. Rate constants are generated over a range of pressures ($P = P_1, P_2, \ldots, P_N$).

$$k_u(T, P_i) = \sum_{j=1}^{M} A_{ij}\, T^{nij} exp(-E_o^{ij}/RT), i\ =\ 1, \ldots, N, M \geq\ 1$$

An extrapolation is bounded by the two pressure limits, P_1 and P_N. To calculate k_u (T, P) for any pressure, log k_u is interpolated as a linear function of log P. If P is between P_i and P_{i+1} for any temperature, a rate constant can be found from:

$$log\ k_u(T, P_i) = log\ k_{u,i} + (log\ P - log\ P_i)\frac{log\ k_{u,i+1} - log\ k_{u,i}}{logP_{i+1} - logP_i}$$

The PLOG formalism is generally superior (more accurate) compared to the TROE formalism if the composition of the gas mixture does not change. However, if the average third body collision efficiency of the mixture significantly changes (e.g. due to the significant increase of the water mole fraction), then the PLOG-based rate coefficient can be erratic.

Notwithstanding the success of the recent small hydrocarbon species mechanisms [64]–[73] there is a continuous need for the community to develop and refine even these small mechanisms. For example, it is well known that the oxidation of ethylene is highly dependent on the rate of reaction of vinyl radicals with molecular oxygen [137]. Prior to 1984 the reaction was generally written as $\dot{C}_2H_3 + O_2 = C_2H_2 + H\dot{O}_2$. However, Slagle et al. [138] found that at low temperatures (< 900 K), the primary products of the reaction were $CH_2O + H\dot{C}O$. Theoretical work [139]–[142] subsequently confirmed the low-temperature chain-propagation pathway, and indicated that another chain-branching pathway forming $\dot{C}H_2CHO + \ddot{O}$ was important at higher temperatures, with the crossover temperature being approximately 900 K. One point to be garnered from this is that it is dangerous to optimize mechanisms when critical features of the PES are still not fully understood.

Most recently, Goldsmith et al. [143] applied a new method to compute the interaction potential for $\dot{R} + O_2$ reactions presenting state-of-the-art calculations of the $C_2H_3\dot{O}_2$ potential energy surface using variable reaction coordinate-, variational- and conventional transition-state theories. Temperature- and pressure-dependent rate coefficients were calculated and confirmed the main product channels to be $CH_2O + H\dot{C}O$ at lower temperatures and $\dot{C}H_2CHO + \ddot{O}$ at higher temperatures with stabilization of $C_2H_3\dot{O}_2$ directly competing with the two product channels at pressures above 10 atm. The decomposition pathways of $C_2H_3\dot{O}_2$ (also calculated) yielded the same dominant pathways, thereby explaining the previous experimental studies' inability to identify the competing stabilization pathway. In addition, Goldsmith et al. calculated the crossover temperatures for the main bimolecular products to be approximately 1000 K at 1 atm, in reasonable agreement with the earlier studies. The advances in quantum chemistry calculations and their relatively high level of accuracy, comparable to, or in excess of experimental measurement for small species in the range C_0–C_4, are invaluable to the development of high-fidelity chemical kinetic models [144].

Despite the success in developing core mechanisms, considerable work remains to be done. A recent study of acetylene oxidation at high pressures and relatively low pressures shows very poor agreement of many common core mechanisms compared to new ignition delay data [145].

Figure 9 shows experimental ignition delay times measured at 10 bar in the NUI Galway shock tube [145] and comparisons with mechanism predictions from GRI-Mech 3.0 [3], San Diego Mech [64], [65], AramcoMech 2.0 [71], [72] and Glarborg Mech [73]. The only model capable of reproducing the data is Glarborg Mech. Analysis of this mechanism indicates that the reaction $C_2H_2 + H\dot{O}_2 \rightarrow \ddot{C}HCHO + \dot{O}H$ is an important contributor to fuel oxidation at high pressures due to the relatively high concentration of $H\dot{O}_2$ radicals. This reaction promotes reactivity by producing two reactive radicals, triplet formyl-methylene and hydroxyl radicals. Formyl-methylene subsequently reacts with molecular oxygen producing $\ddot{O}$ atoms which further promote reactivity. This reaction was published by Gimenez-Lopez et al. [146], but is not included in the other mechanisms. Without this calculation, the effect of $C_2H_2 + H\dot{O}_2$ would be considered very small due to the high activation energy of the reaction $C_2H_2 + H\dot{O}_2 \rightarrow \dot{C}_2H$

+ H_2O_2. Thus, it is recommended that the community adopt a systematic approach to accurately determining the potential energy surfaces (PESs) of important reactions so that we can develop more accurate, high-fidelity models. As mentioned earlier KinBot [119] has been developed to do just this.

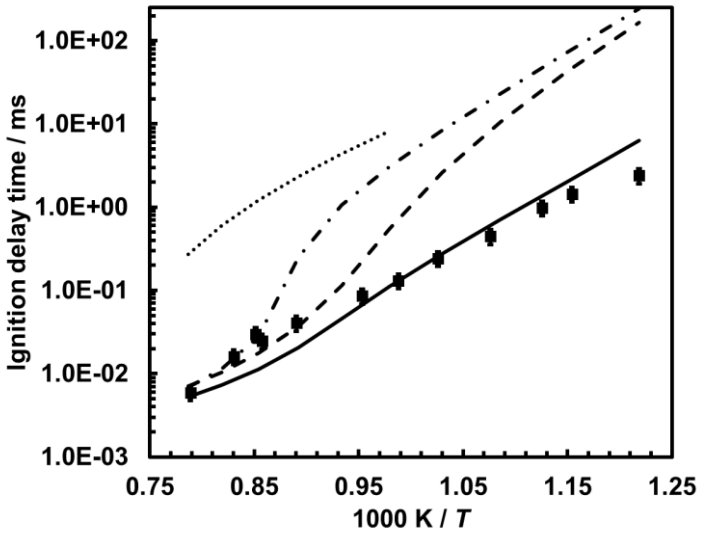

Fig. 9: Acetylene IDT at φ = 1.0 in air at P = 10 bar. Experimental results (symbols), constant volume simulations (lines) of four different models from the literature [145]. Solid line – Glarborg Mech [73], dashed line – AramcoMech2.0 [71], [72], dotted line – GRI-Mech 3.0 [3], dash-dotted line – San Diego Mech [64], [65].

4.2 Lumped and semi-empirical models

Probably the most successful lumped mechanisms stem from the CRECK modelling group of Ranzi and Faravelli [69]. The general concept was first published by Ranzi et al. in 1983 [147] in which the high-temperature mechanism for *n*-heptane pyrolysis included detailed H-atom abstraction, isomerization and β-decomposition reactions. A kinetic post-processor, SPYRO Program, generated a single lumped reaction for the equivalent high-temperature decomposition of the 'lumped radical' mixture $\dot{C}_7H_{15}$ [148], [149]. This is reasonable as the timescale for decomposition of such a radical at T > 1000 K is ~ 1 μs. For example, at 1040 K the $\dot{C}_7H_{15}$ radical decomposition products = 0.0211 $\dot{H}$ + 0.0806 $\dot{C}H_3$ + 0.2297 $\dot{C}_2H_5$ + 0.3629 1-$\dot{C}_3H_7$ + 0.3057 1-$\dot{C}_4H_9$ + 0.2277 C_2H_4 + 0.3463 C_3H_6 + 0.2705 C_4H_8 + 0.1912 C_5H_{10} + 0.0806 C_6H_{12} + 0.0189 C_7H_{14}. At different temperatures, the product set is the same but different fractions of the species are produced in the 'lumped reactions'. In this way a very complex mechanism involving hundreds to thousands of species and thousands of reactions can be simplified to reduce the computational requirements needed for use of mechanisms in numerical models. Ranzi et al. also applied this method to the low temperature mechanism of *n*-pentane for the automatic generation of primary oxidation reactions and lumping procedures [150].

The semi-empirical approach was proposed by Axelsson et al. [151] and used in a more simplified form by Warnatz [152]. It assumes that the dominant route of fuel consumption is abstraction of a hydrogen atom by smaller radical species (e.g. $\dot{H}$, $\dot{O}$, $\dot{O}H$) leading to the formation of a fuel radical. The principal empiricism lies in the description of the fuel radical decomposition into smaller products, e.g. $\dot{C}_7H_{15} \rightarrow \dot{C}H_3 + 2C_3H_6$ in the Warnatz model for *n*-heptane [152]. A simplified propene mechanism neglected abstraction reactions by considering only four radical addition reactions. The remainder of the mechanism included core C_0–C_2 species and reactions. This type of approach was developed further by Held et al. [153] who

also studied *n*-heptane pyrolysis and oxidation by considering three types of reaction for primary fuel consumption; (i) thermal decomposition, (ii) H-atom abstraction by an active radical (Ḣ, Ö, ȮH, $H\dot{O}_2$, $\dot{C}H_3$, $\dot{C}_3H_5$) and (iii) decomposition of the alkyl radicals formed. This method was successfully adopted by Held et al. to simulate a wide range of independent data sets including species profiles versus time measured in a flow-reactor, species versus temperature profiles measured in a jet-stirred reactor, ignition delay time measurements and flame speed measurements.

The general concept of lumped and semi-empirical mechanism has recently been employed by Xu et al. in the development of a hybrid chemistry HyChem [154] approach for application to petroleum-derived jet fuels—essentially high-temperature combustion. This approach decouples fuel pyrolysis from the oxidation of fuel decomposition intermediates, similar to the approach outlined by Held et al. [153]. The thermal decomposition and oxidative thermal decomposition processes are simulated using seven lumped reaction steps in which the stoichiometric and reaction rate coefficients may be derived from experiments, again similar to the lumping procedure by Ranzi et al. [147].

The temperatures and timescales are such that the mechanism can be broken down by:

$$C_mH_n = e_d(C_2H_4 + \lambda_3C_3H_6 + \lambda_{4i}i\text{-}C_4H_8 + \lambda_{4n}1\text{-}C_4H_8) + b_d[\chi C_6H_6 + (1-\chi)C_7H_8] + \alpha H + (2-\alpha)CH_3$$

$$\text{and } C_mH_n + \dot{R} = RH + \gamma CH_4 + e_a(C_2H_4 + \lambda_3C_3H_6 + \lambda_{4i}i\text{-}C_4H_8 + \lambda_{4n}1\text{-}C_4H_8) + b_a[\chi C_6H_6 + (1-\chi)C_7H_8] + \beta H + (1-\beta)CH_3$$

where $\dot{R}$ = Ḣ, $\dot{C}H_3$, Ö, ȮH, O_2 and $H\dot{O}_2$. The stoichiometric parameters α, β, and χ are bounded, $\alpha \in [0,2]$, $\beta \in [0,1]$ and $\chi \in [0,1]$. In addition, e_d, e_a, b_d and b_a are dependent variables because of elemental conservation. Among the independent stoichiometric parameters, λ_3 is the C_3H_6-to-C_2H_4 ratio; λ_{4i} and λ_{4n} are the ratios of *iso*-C_4H_8- and 1-C_4H_8-to-C_2H_4, respectively; χ is the ratio of C_6H_6 to the sum of C_6H_6 and C_7H_8; α and β are largely related to the rates of production of the Ḣ atom, C_2H_4 and CH_4; γ is the CH_4 yield in addition to H-abstraction by $\dot{C}H_3$.

The product species included are methane, ethylene, propene, 1-butene, *iso*-butene, benzene and toluene in addition to hydrogen atoms and methyl radicals. The oxidation process is described by detailed chemistry of foundational hydrocarbon fuels. Results were obtained for three petroleum-derived fuels: JP-8, Jet A and JP-5 as examples. The experimental observations show only a small number of intermediates are formed during thermal decomposition under pyrolysis and oxidative conditions and support the hypothesis that the stoichiometric coefficients in the lumped reaction steps are not a strong function of temperature, pressure, or fuel-oxidizer composition. Modeling results demonstrated that HyChem models can predict a wide range of combustion properties at high temperatures, including ignition delay times, laminar flame speeds, and non-premixed flame extinction strain rates of all three fuels.

4.3 Intermediate temperature chemistry

As illustrated in Fig. 5 above, the small species chemistry controls most high temperature (> 1200 K, depending on pressure) oxidation phenomena, particularly flame speed predictions and has a very strong influence on ignition delay time predictions. Later, there will be a discussion of low temperature chemistry, typically in the range 600–850 K. Intermediate temperature chemistry generally occurs in the temperature range 850–1200 K. The important reactions are:

$$\dot{H} + O_2\,(+M) = H\dot{O}_2\,(+M)$$
$$R\dot{O}_2 = \text{olefin} + H\dot{O}_2$$

$$RH + H\dot{O}_2 = \dot{R} + H_2O_2$$
$$H_2O_2\,(+M) = \dot{O}H + \dot{O}H\,(+M)$$

At intermediate temperatures copious quantities of hydroperoxyl ($H\dot{O}_2$) radicals are formed by the reaction of hydrogen atoms with molecular oxygen in addition to the concerted elimination reaction ($R\dot{O}_2$ = olefin + $H\dot{O}_2$). Sensitivity analyses at intermediate temperatures and high pressures (> 10 atm) typically highlight the importance of fuel + $H\dot{O}_2$ radical reactions, e.g. Fig. 10(a).

Rate constants for concerted elimination reactions are not well known. Indeed, there had been a lot of controversy around this reaction as to whether or not it proceeds via a concerted elimination as $R\dot{O}_2$ = olefin + $H\dot{O}_2$, or whether the alkyl-peroxyl radical first undergoes an internal hydrogen atom isomerization, leading first to the formation of a hydroperoxyl-alkyl radical ($\dot{Q}OOH$), followed by decomposition to olefin + $H\dot{O}_2$ radical. Using quantum chemistry calculations Quelch et al. [155] first proposed that the reaction $\dot{C}_2H_5 + O_2$ reacts through a cyclic transition state, proceeding directly to $C_2H_4 + H\dot{O}_2$ through a concerted elimination reaction, and that it did not proceed through the $\dot{Q}OOH$ radical. These calculations supported the work of Baldwin and Walker [156], [157] who proposed that a pathway involving a quasi-stable structure must exist without the prior formation of $C_2H_5\dot{O}_2$, which can decompose to $C_2H_4 + H\dot{O}_2$.

Recent accurate theoretical calculations [158]–[160] and experimental studies e.g. [161], [162], show that the major pathway for $H\dot{O}_2$ formation is the direct elimination of $H\dot{O}_2$ from $R\dot{O}_2$ radicals. These reactions have also recently been studied in a systematic way by Villano et al. [163], [164] and Miyoshi [165], [166] using quantum chemistry calculations at varying levels of theory to help develop rate rules for alkyl + O_2 reactions at lower temperatures. The more comprehensive study was performed by Villano et al. [163] where rate constants were calculated for 23 different C_2–C_6 straight-chained and branched alkyl-peroxyl radicals. Separate rate rules were recommended for straight-chained and less-branched radicals and those leading to more highly substituted olefins.

Although Jemi-Alade et al. [167] have measured the rate constant of $H\dot{O}_2$ with CH_2O in a flash photolysis study, there have been few direct experimental measurements of the rates of H-atom abstraction reactions by $H\dot{O}_2$ radicals due to the lack of a suitable radical precursors. Walker et al. e.g. [168], [169] have also made indirect relative rate measurements with the most recent recommendations (2002) for rate of abstraction from alkanes, aromatics and related compounds [170]. Indeed, it has only been in recent years that methods have been developed to quantitatively measure $H\dot{O}_2$ radicals using the FAGE (Fluorescence assay by Gas Expansion) technique [171], dual-modulation Faraday spectroscopy [172], [173] and cavity ring-down spectroscopy [174]. It would be a considerable development for the community if it became possible to measure rates of H-atom abstraction reactions by $H\dot{O}_2$ radicals from stable molecules. Due to the lack of experimental measurements, recent efforts have been made to calculate rate constants using quantum chemistry for alkane fuels [175]– [177] in addition to oxygenated species [178]–[183]. In the case of the alkane fuels studied, overall good agreement was observed between the rate constants calculated by Aguilera-Iparraguirre et al. [177] and those recommended by Scott and Walker [170] for small molecules up to butanes. Further work is recommended for larger alkanes. Some uncertainty remains for oxygenated species. By performing a global uncertainty analysis of methanol oxidation, Klippenstein et al. [183] attributed the deficiency in predicting ignition delay times to the rate constant for the reactions of methanol with $H\dot{O}_2$ radicals.

In 2011, three papers were published where high-level quantum chemistry calculations were performed by Altarawneh et al. [183], Alecu and Truhlar [184] and Klippenstein et al. [185].

The values calculated in these studies varied by almost an order of magnitude from the slowest rate constant from Klippenstein et al. to the fastest value by Altarawneh et al., with that calculated by Alecu and Truhlar falling approximately midway between the other two, Fig. 10(b). There are two main issues. The first is that there is such a wide range of disagreement among the calculations and the second is that the reaction is so important to the prediction of almost all existing methanol validation targets as indicated by Klippenstein et al. [185]. Note that the fastest calculated rate constants, i.e. those from Altarawneh et al. tend to agree better with the wide range of validation data present in the literature [186], [187]. Discussions with the authors of these studies indicated that there were no apparent errors in the calculations as presented. Furthermore, Alecu and Truhlar [184] attributed the difference between their calculations and those of Klippenstein et al. to different treatments of anharmonicity. This difference in calculated values is worrying, particularly as the calculated rate constant from Klippenstein et al. is approximately an order of magnitude slower compared to the 'optimized' value (solid line in Fig. 10(b)) from Olm et al. [186] and lies at the edge of their posterior uncertainty range. The apparent discrepancy may point to a contribution of a chemically activated reaction involving $H\dot{O}_2$ radicals, rather than the reaction being completely thermally controlled. These discrepancies also indicate the need for improvements in theoretical methods.

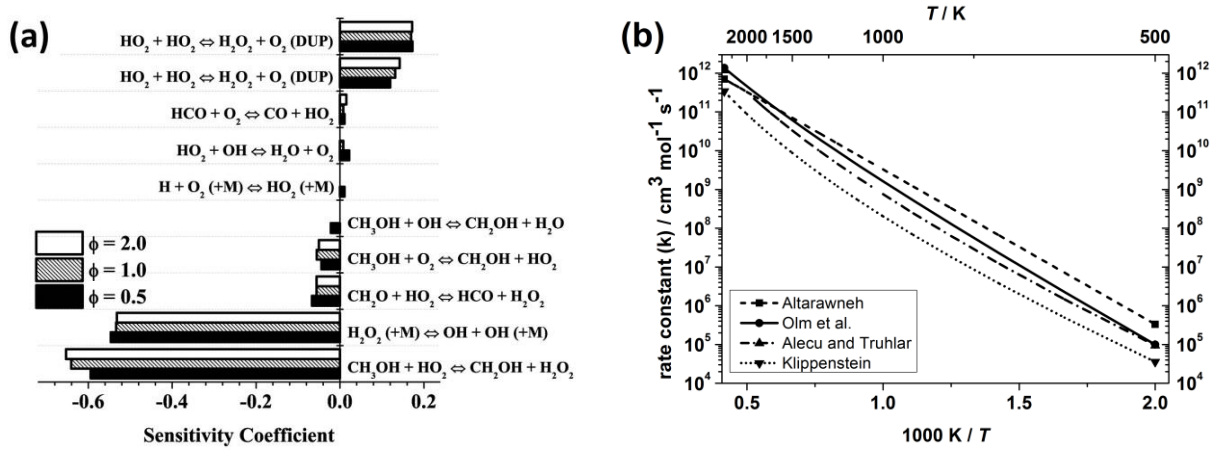

Fig. 10: (a) Sensitivity coefficients to changes in ignition delay times resulting from factor of two changes in A-factor for reactions pertaining to CH_3OH oxidation at 8.55% O_2, P = 40 atm and T = 885 K [187]. (b) Temperature dependent rate constants for the reaction $CH_3OH + H\dot{O}_2 \rightarrow \dot{C}H_2OH + H_2O_2$. Dashed line – Altarawneh *et al*. [183], dash-dotted line – Alecu and Truhlar [184], dotted line – Klippenstein et al. [185], solid line – Olm et al. [186].

Another important radical abstractor at intermediate temperatures is the methyl-peroxy ($CH_3\dot{O}_2$) radical, which is typically seen as being important in the decomposition of species which produce high concentrations of methyl radicals including branched alkanes, e.g. iso-octane [5], and methane/dimethyl ether and their mixtures [188]. Sensitivity is typically observed to the rate of H-atom abstraction from the fuel by $CH_3\dot{O}_2$ radicals through the following sequence of reactions:

$$\dot{C}H_3 + O_2 = CH_3\dot{O}_2$$
$$RH + CH_3\dot{O}_2 = \dot{R} + CH_3O_2H$$
$$CH_3O_2H = CH_3\dot{O} + \dot{O}H$$

Carstensen et al. [175], [176] used quantum chemistry to calculate rate constants for H-atom abstraction from alkanes by a series of $R\dot{O}_2$ radicals, including $CH_3\dot{O}_2$. There are very few studies of H-atom abstraction by $CH_3\dot{O}_2$ radicals and further efforts are recommended.

4.4 Low temperature chemistry

At low temperatures (450–850 K) the chemistry is quite complex where chain branching stems from the addition of fuel radicals to molecular oxygen in the sequence of reactions: $\dot{R} + O_2 \rightarrow R\dot{O}_2 \rightleftharpoons \dot{Q}OOH + O_2 \rightarrow \dot{O}_2QOOH \rightleftharpoons HO_2\dot{Q}OOH \rightarrow R\dot{O} + \dot{O}H + \dot{O}H$. A general reaction scheme for low temperature oxidation is provided in Fig. 11.

The underlying chemistry was first discussed by Knox [189] and Fish [190], with further understanding and improvements made by Pollard [191], Cox and Cole [192], Hu and Keck [193] Walker and Morley [194] and Griffiths et al. [195]. A good review of the kinetics of elementary reactions in low-temperature oxidation chemistry was published by Zádor et al. [196] and some dedicated quantum chemistry studies have been performed to help develop these rate rules [163]–[166], [197], [198]. At low temperatures the fuel undergoes H-atom abstraction generating alkyl radicals ($\dot{R}$) which add to molecular oxygen, forming alkyl-peroxyl ($R\dot{O}_2$) radicals. These undergo a unimolecular H-atom isomerization, generating hydroperoxyl-alkyl ($\dot{Q}OOH$) radicals. It is the fate of these $\dot{Q}OOH$ radicals that contributes significantly to negative temperature coefficient (NTC) behavior.

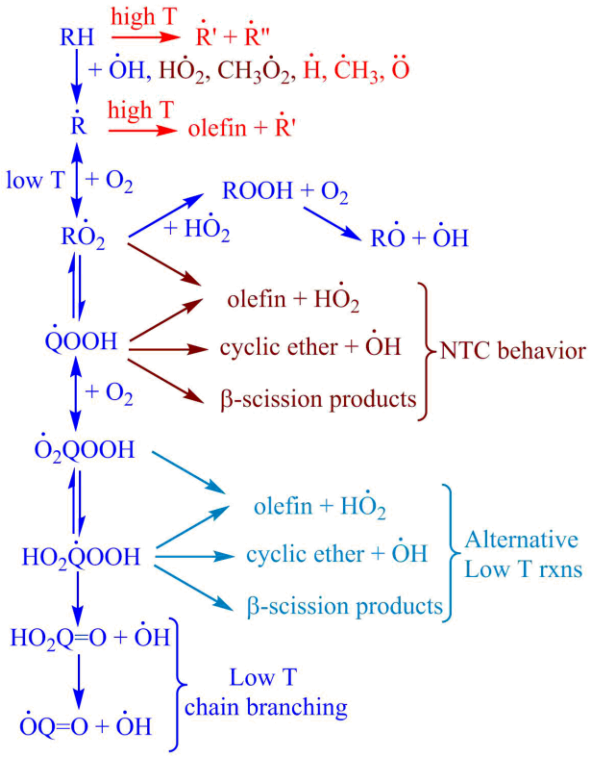

Fig. 11. General schematic mechanism for fuel oxidation.

At low temperatures (600~750 K) $\dot{Q}OOH$ radicals add to molecular oxygen, producing peroxy-hydroperoxyl-alkyl ($\dot{O}_2QOOH$) radicals, which can undergo internal H-atom isomerization forming $HO_2\dot{Q}OOH$ radicals. These can decompose to generate a carbonyl-peroxide species and a hydroxyl ($\dot{O}H$) radical. The cleavage of the O–O bond in this peroxide produces two radicals, a carbonyl-alkoxy radical and another $\dot{O}H$ radical. Overall, this process is chain-branching as a fuel radical formed via H-atom abstraction by $\dot{O}H$ radicals leads to the formation of three (one carbonyl-alkoxy and two $\dot{O}H$) radicals. This behavior persists in the temperature range 600–700 K. However, at higher temperatures the activation energy barriers for the propagation reactions from $\dot{Q}OOH$ radicals leading to the formation of cyclic ethers and other β-scission products, in addition to the concerted elimination of an olefin and $H\dot{O}_2$ radicals

from $R\dot{O}_2$ species can be overcome, resulting in NTC behavior as just one radical species is formed rather than three radicals via the chain-branching process.

Note that further additions to molecular oxygen are possible, evidence of which were detected in recent work performed by Wang et al. [199], [200] at Lawrence Berkeley National Laboratory/Sandia National Laboratory.

Due to the complexity of the kinetics of fuel oxidation and particularly of the low temperature reaction scheme, it has become customary to describe fuel oxidation using a series of reaction classes, e.g. (1) unimolecular fuel decomposition, (2) H-atom abstraction from the fuel, (3) fuel radical decomposition, etc. In Curran et al. [4] rate rules were developed for 25 high- and low-temperature reactions. Recently, the work by Bugler et al. [125], [201], extended this to include 31 different reaction classes with associated rate constants to describe the low temperature oxidation of the pentane isomers. This work validated the community's general understanding of low temperature chemistry as applied to alkane fuels [189]–[195] and the model was also successfully used to simulate important intermediate species produced during the oxidation of *n*-pentane [202]. This body of work was significant in that the thermodynamic parameters of the low temperature species (alkyl-peroxides, carbonyl-peroxides and their radicals) were re-calculated based on a review by Burke et al. [203] where group additivity values were optimized taking reliable data published in the literature. At the same time, the most recent measured and calculated rate constants for the most important reactions in the low-temperature reaction scheme were used in the model with significant success. Subsequently, Cai et al. [204] built upon the work of Bulger et al. and developed rate rules for C_7–C_{11} *n*-alkanes and used the rate rules so optimized to develop a mechanism to describe *n*-dodecane oxidation (C_{12}) which successfully simulated experimental ignition delay times. These have also recently been applied to the branched alkane, *iso*-octane [205], and it is intended that future work will include many more branched alkanes so that high-fidelity kinetic mechanisms for all alkanes can be accurately generated using fundamentally based thermochemistry and kinetic rate parameters.

Thereafter, mechanisms describing the oxidation of other fuels such as olefins (alkenes, dienes, etc.) can be accurately developed. We can then expand this knowledge to include fuels with functional groups such as alcohols, ethers, esters, aldehydes, ketones, acids, etc. Many of these fuels contain alkyl chains similar to alkanes and so many of the reactions and rate constants pertinent to alkanes are also applicable to other fuels. Moreover, oftentimes the mechanisms are naturally inter-dependent. In the low-temperature oxidation of alkanes, alkenes (olefins) are produced, particularly via the sequence $R\dot{O}_2 \rightarrow$ olefin + $H\dot{O}_2$. Furthermore, at low temperatures the addition of a hydroxyl radical to olefinic species leads to the formation of α-hydroxy-alkylperoxyl radicals, which are important primary radicals produced via H-atom abstraction from alcohols. Thus, the low-temperature oxidation mechanisms of alkanes, alkenes and alcohols are all inter-linked.

Of course, there are differences. It is well known that alcohols are less reactive than their corresponding alkane, e.g. *n*-pentanol has a higher RON = 80 [206] and is thus slower to ignite compared to *n*-pentane, RON = 61.7 [207]. It is known that in alcohols the hydrogen atom bonded to the carbon alpha to the –OH alcohol functional group is weaker than all others due to electron delocalization and thus abstraction from this site will be faster and hence relatively more α-hydroxy-alkyl radicals are formed from alcohols compared to others, see Sarathy et al. [208]. Da Silva et al. [209] used quantum chemistry calculations to study the reaction of α-hydroxy-ethyl radicals with O_2 and found that the α-hydroxy-ethylperoxyl radical undergoes a concerted elimination reaction, with a barrier of only 11.4 kcal mol^{-1}, leading to the formation of acetaldehyde and $H\dot{O}_2$, Fig. 12.

This leads to an inhibition of the low-temperature reactivity, as it results in propagation rather than chain-branching as discussed by Sarathy et al. [210] in their butanol isomer study. This type of reaction is similarly important for all other alcohols as discussed in the review by Sarathy et al. [208] showing a correlation between RON and ignition delay time which is due to the prevalence of this concerted elimination pathway leading to the formation of an aldehyde/ketone + $H\dot{O}_2$ radical.

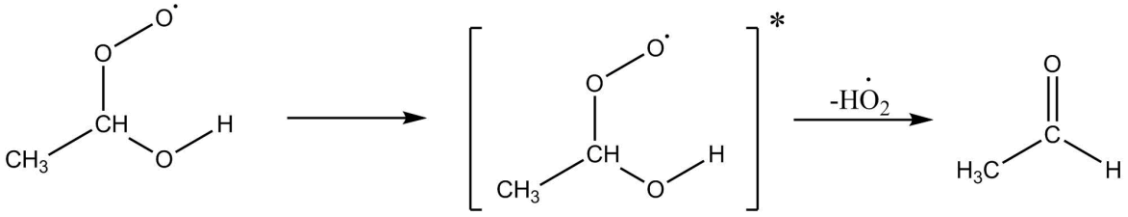

Fig. 12. Formation of aldehyde from alcohol as proposed by da Silva et al. [209].

Developing chemical kinetic mechanisms in a systematic way and using rate rules is not new or unique. In 1975 Halstead et al. [211] published the Shell model to simulate the low-temperature oxidation of large alkanes. This was a generalized model including initiation, chain propagation, degenerate branching and termination steps with kinetic parameters fitted empirically. Subsequently, Cox and Cole [192], Hu and Keck [193] Walker and Morley [194] and Griffiths et al. [195] developed short/simple mechanisms involving globalized species and elementary reaction steps. Ranzi and Faravelli had similar success in developing semi-detailed mechanisms using their automatic generator of reactions (MAMOX) code applied to the oxidation of alkanes [148], particularly the primary reference fuels *n*-heptane [212] and *iso*-octane [213].

Chevalier et al. [214]–[216] were among the first to describe the computer-aided automatic generation of reaction mechanisms for large aliphatic hydrocarbon fuel molecules, including *n*-heptane, *n*-decane and *n*-hexadecane but reaction details were not included in their publications. Reaction rate details were subsequently published by Curran et al. in their work on *n*-heptane [4] and *iso*-octane [5] where 25 different classes of reaction were included in mechanisms generated by hand. Morley [217] and Blurock [218] developed software to generate low-temperature oxidation mechanisms for linear and branched alkanes. The REACTION software developed by Blurock was enhanced by Moréac et al. [219] to develop a mechanism for *n*-heptane and *n*-decane using the reaction classes proposed by Curran et al. [4],[5]. Battin-Leclerc's group developed EXGAS [220] for the automatic generation of kinetic models based on initial work by Haux et al. [221],[222]. This mechanism includes a comprehensive core C_0–C_2 reaction base with a lumped secondary mechanism developed using the KINGAS software [223]. The thermodynamic parameters for each species are produced using THERGAS [224]. Similarly, Gent University have developed Genesys [225], [226] a kinetic model construction tool, for use in conjunction with chemo-informatics libraries, which employs a rule-based network generation methodology. This includes a Benson group additivity method [227] for the estimation of thermodynamic parameters and a kinetic group additivity scheme for the estimation of Arrhenius parameters.

The Reaction Mechanism Generator (RMG) [228] developed by Green and West at MIT and Northeastern University is an open source, automatic chemical reaction mechanism generator that constructs kinetic models composed of elementary reaction steps using an understanding of how molecules react. It has been commonplace in the community to provide a mechanism file and a species thermodynamic list in NASA polynomial format with mechanisms. However, it is not always easy to identify individual chemical structures from species names. For example, in the LLNL/NUIG mechanisms the species $nC_7H_{14}OOH2\text{-}4$ and $nC_7H_{14}OOH4\text{-}2$ are distinct molecules but without some way to identify the species molecular composition a user

cannot identify the individual molecules. Considering this, species glossaries are (sometimes) provided to help the user identify the molecular structure of individual species, e.g. [201].

The community has not yet adopted a common approach to unique species identifiers, but options are available. The simplified molecular-input line-entry system (SMILES) [229] is a linear text format to describe the connectivity and chirality of a molecule. A canonical SMILES string provides a single 'canonical' form of a molecule. Similarly, the IUPAC International Chemical Identifier (InChI string) developed by IUPAC and NIST from 2000–2005 [230], [231] aims to provide a unique, or canonical, identifier for chemical structures and to facilitate the search for such species in databases and on the web. A CAS registry number is a unique numerical identifier assigned by the Chemical Abstracts Service (CAS) [232] to every chemical substance described in the open literature. The RMG software includes the ability to search for molecules using any species identifier, such as SMILES, InChI, or CAS number or species name in the 'species identifier' field. Species identification is important for the user in understanding the chemical pathways leading to and from individual species. However, to date most models developed do not include SMILES/InChI/CAS numbers for species listed in reaction mechanism and/or thermochemistry files. It would be useful to the community if one or more forms of these identifiers are adopted so that species can be readily identified, and associated thermochemistry and reactions can be cross-checked.

There are many oxygenated species produced during the low temperature oxidation process, which depend on the parent fuel structure, and thermodynamic parameters are needed for these. It is impractical to consider using high-level quantum chemistry calculations to derive accurate thermochemical parameters of molecules larger than C_8 with oxygenated groups attached. To calculate the thermochemistry of these species the group at Nancy developed THERGAS [224]. This code is based on Benson's group additivity method [227] in which each group centered on a heavy atom contributes to the enthalpy, entropy and heat capacity of a molecule. By defining the local environment around each heavy atom and summing the contributions of each and taking symmetry into account the thermochemistry of a molecule can be calculated. The THERM code developed by Ritter and Bozzelli [233] uses the same principle and a similar tool is available as a NIST group additivity program [234] and Cranium which is a component software for physical property estimation available on the internet [235] from Molecular Knowledge Systems.

It has previously been shown that kinetic predictions are sensitive to the thermochemical parameters of species [236]–[238]. The recent work by Bugler et al. [199] showed the importance of the thermochemistry of the species involved in the low-temperature oxidation of the pentane isomers. Figure 13 shows the influence on predicted ignition delay times—there is approximately an order of magnitude difference in predictions (black line compared to the red line) in up-dating the thermodynamic parameters of the low temperature oxygenated species associated with *n*-pentane compared to that used in the PRF studies [4], [5]. Details of the changes are provided by Bugler et al. [201] but it is obvious that accurate thermochemistry of the low-temperature oxygenated species have a very significant influence on model predictions of fuel reactivity. This is an area of considerable neglect by the community where relatively few studies have been performed on large oxygenated molecules.

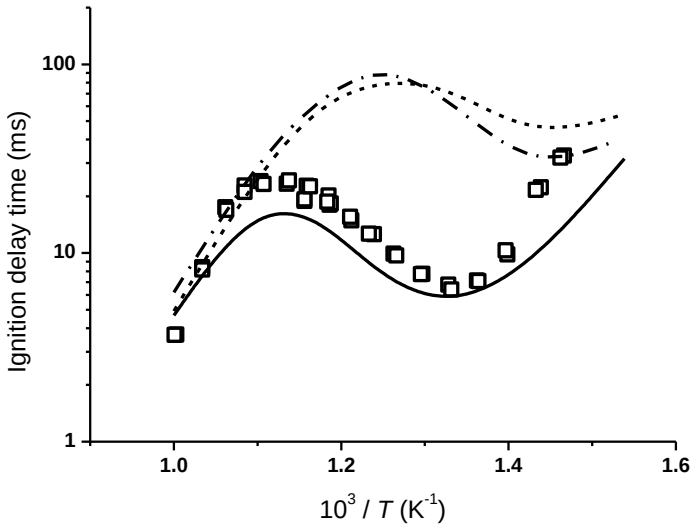

Fig. 13. Effect of updated thermochemistry and sub-mechanism on *n*-pentane oxidation, φ = 1.0 in "air", 10 atm reported by Bugler et al. [201]. Symbols represent IDTs from an RCM. Solid line – model predictions using original thermochemistry; dashed line – model predictions using updated thermochemistry; dash-dotted line – model predictions using updated thermochemistry and C_0–C_4 sub-mechanism [70], [88], [187], [239], [240]. All simulations shown are at constant volume conditions.

Since chemical kinetic mechanisms require accurate knowledge of the thermodynamic properties of the species involved care must be taken in compiling these data. There are a number of on-line resources available. The NIST Webbook database [241] provides a compilation of thermodynamic and physical property data for chemical species available from the literature. The Third Millennium Ideal Gas and Condensed Phase Database for Combustion developed by Burcat and transferred to Goos is also available online [242]. Probably, the most accurate and the current benchmark for heats of formation (ΔH^0_f), certainly for small species, are the Active Thermochemical Tables (ATcT) [243] available from Ruscic et al. [244]–[248]. ATcT is based on constructing, analyzing and solving an underlying Thermochemical Network (TN) to develop accurate, reliable, and internally consistent thermochemical values for species. Many experimentally measured values are considered, and in their recent publication, both high-level ab initio calculations combined with the ATcT approach were used to produce heats of formation of a set of 348 C, N, O, and H containing species with estimated 2σ uncertainties in the range of ±1.0–1.5 kJ mol^{-1} [248]. This is excellent progress for the community, certainly for heats of formation. However, accurate entropy and heat capacity values are also needed so that Gibbs free energy values are available for accurate thermochemical equilibrium calculations. It can be expected that further calculations of similar and larger species to those performed by Klippenstein et al. [248] will be available in the future, and efforts such as the ATcT initiative should be extended to also include these. The community would benefit greatly from such an eventuality. Indeed, Keceli et al. [121] have developed automated computational thermochemistry values describing the species involved in butane, presented at this symposium. It is acknowledged that, for the foreseeable future, there will be a trade-off between molecular size and accuracy of the quantum chemistry calculations that can be performed for molecules. Thus, into the future there will continue to be a need to develop accurate Benson group values so that reasonably accurate thermodynamic parameters for large (> C8) hydrocarbon and oxygenated hydrocarbon species can be produced. This will contribute considerably to the continued development of mechanism with consistent rate rules describing

the oxidation for all fuels including straight-chained and branched alkanes, olefins, alcohols, ethers, esters, etc.

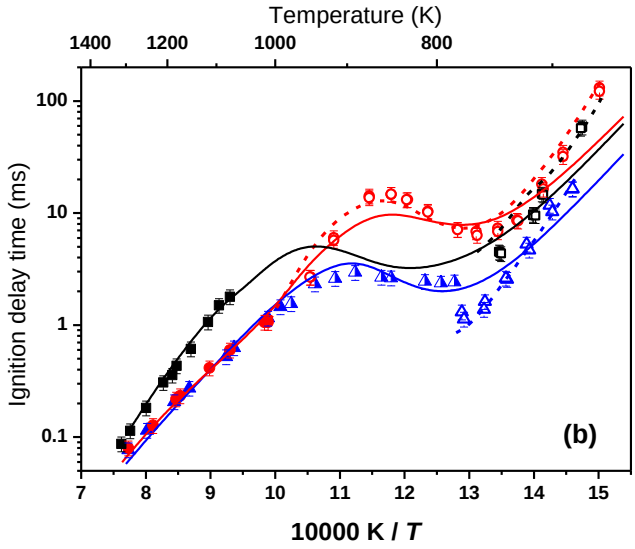

Fig. 14: Plots of experimental (points) and predicted (lines) for pentane isomer oxidation, φ = 1.0 in air, P = 20 atm; △, ▲, ◮ – *n*-pentane, ○, ● – *iso*-pentane, □, ■ – *neo*-pentane. Solid lines are constant volume simulations, dashed lines include facility effects. Reproduced from Bugler et al. [125] with permission from Elsevier.

Having discussed the importance of thermochemistry, let us now consider the important reactions by exploring the comparative reactivities of the pentane isomers. Figure 14 shows a plot of experimentally measured ignition delay times and corresponding model predictions for the oxidation of the pentane isomers (*n*-, *iso*- and *neo*-pentane) for stoichiometric fuel in air mixtures at a pressure of 20 atm. At the lowest temperatures (~600–650 K) the reactivity of all three fuels are similar (see also Fig. 7). At even lower temperatures (< 600 K), the activation energy of approximately 43 kcal mol^{-1} leading to the decomposition of stable carbonyl hydroperoxide ($HO_2Q{=}O$) species cannot be overcome and so they accumulate. There comes a threshold in temperature in the range 600–650 K where the rate of the reaction $HO_2Q{=}O$ = $\dot{O}Q{=}O$ + $\dot{O}H$ starts to become significant due to both the increased temperature at which the activation energy barrier for O–OH bond cleavage can be overcome and the increasing concentration of $HO_2Q{=}O$ molecules, which also contributes to an increase in reaction rate. In the temperature range 650–1000 K, *n*-pentane is fastest to ignite while *iso*-pentane is the slowest with *neo*-pentane being intermediate in reactivity compared to the other two.

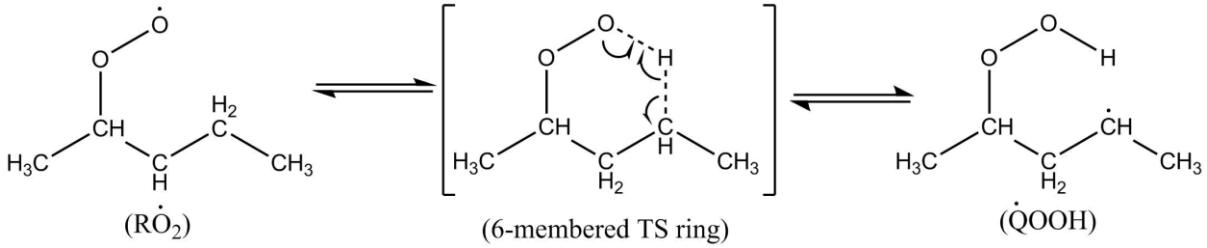

Fig. 15. Facile six-membered transition state from an alkyl-peroxyl ($R\dot{O}_2$) to a hydroperoxyl-alkyl ($\dot{O}OOH$) radical in *n*-pentane.

At higher temperatures *n*-pentane and *iso*-pentane show almost identical ignition times, with *neo*-pentane being considerably slower compared to the other two. This behavior has been discussed previously by Bugler et al. [125]. Briefly, in the temperature range 650–1000 K *n*-pentane and *iso*-pentane show similar reactivity profiles in that the logarithm of ignition delay time varies linearly with temperature in the temperature range 650–750 K, it shows an NTC

behavior in the temperature range 750–900 K, and increases exponentially with temperature again at temperatures above 900 K. However, there is almost an order of magnitude difference in reactivity between the two fuels in the NTC region, with *n*-pentane being much faster to ignite compared to *iso*-pentane. This is due to the predominance of the formation of relatively low activation energy six-membered transition state rings in the oxidation of *n*-pentane compared to *iso*-pentane, Fig. 15.

It is well known that abstraction of secondary hydrogen atoms compared to primary ones is easier due to their lower bond dissociation energy (BDE) and there are six secondary (and six primary) hydrogen atoms in *n*-pentane compared to just two secondary and nine primary hydrogen atoms in *iso*-pentane. Even though abstraction by ȮH radicals is not very dependent on BDE the rate constant does follow the order $3^o > 2^o > 1^o$. More significantly, the subsequent internal H-atom isomerization reactions, e.g. Fig. 15, leading ultimately to low-temperature chain-branching, have lower activation energy barriers for secondary hydrogen atoms compared to primary one, and are thus relatively faster.

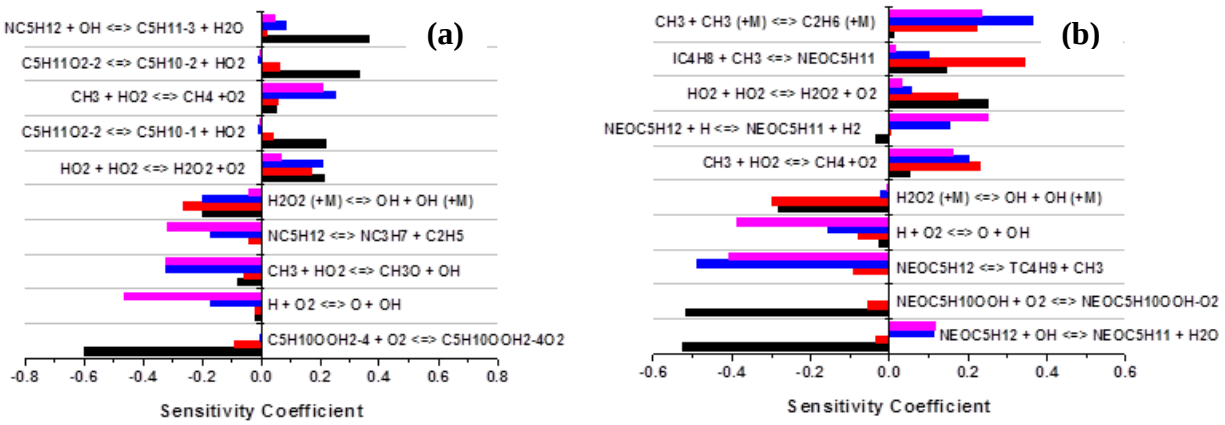

Fig. 16. Sensitivity coefficients to changes in ignition delay times resulting from factor of two changes in A-factor for reactions pertaining to (a) *n*-pentane and (b) *neo*-pentane, φ = 1.0 in 'air', P = 10 atm, at T = ■ 750 K, ■ 950 K, ■ 1150 K, and ■ 1350 K. Reproduced from Bugler et al. [125] with permission from Elsevier.

Examples of sensitivity analyses to (a) *n*-pentane and (b) *neo*-pentane ignition delay times, derived from [125], are provided in Fig. 16. Both figures show the five most important reactions promoting and inhibiting reactivity at the four different temperatures. The reactions of significant importance are (i) hydrogen atom abstraction from the fuel by hydroxyl radicals, (ii) concerted elimination reactions of the *n*-pentyl peroxyl radicals to form 1- and 2-pentene and HȮ$_2$ radicals (this reaction class is not possible for *neo*-pentane), (iii) the addition of hydroperoxyl-pentyl (ȮOOH) radicals (Ċ$_5$H$_{10}$OOH2-4 and neoĊ$_5$H$_{10}$OOH) to molecular oxygen to form peroxyl-hydroperoxyl-pentyl radicals (C$_5$H$_{10}$OOH2-4Ȯ$_2$ and neoC$_5$H$_{10}$OOH2-Ȯ$_2$), ultimately leading to low-temperature chain-branching. Note that the concerted elimination reactions are propagating and thus inhibit reactivity, while ȮOOH radical addition to molecular oxygen ultimately leads to chain branching and thus promote reactivity. The competition between propagation and branching results in the observed negative temperature coefficient (NTC) behavior of alkane fuels at low to intermediate temperatures. Moreover, because no concerted elimination reaction is possible for *neo*-pentane there is a weaker NTC behavior observed in its oxidation relative to *n*-pentane and *iso*-pentane.

Given their apparent sensitivity, rate constants for H-atom abstraction from alkanes by hydroxyl radicals have been measured experimentally, earlier studies were performed by Tully et al. [250]–[254] and Bott and Cohen [255]–[258] with more recent measurements by Farooq

et al. [259]–[261] and correlations based on a group-additivity transition state-theory model were developed by Cohen [262] and updated by Sivaramakrishnan and Michael [263]. There is evidence that group-additivity correlations work well based on the comparisons of the measurements of rate constants for H-atom abstraction from propane and *n*-butane by ȮH radicals measured by Badra et al. [259] compared to the measurements and group-additivity correlations provided by Sivaramakrishnan and Michael [263].

Rate constants associated with the concerted elimination reaction, $R\dot{O}_2$ = olefin + $H\dot{O}_2$, are discussed in Section 4.3 above and were systematically calculated by Villano et al. [163], [164] and Miyoshi [165], [166]. As part of their quantum chemistry calculations of alkyl + O_2 reactions at lower temperatures, they also reported on $R\dot{O}_2 \rightleftharpoons \dot{Q}OOH$ isomerization reactions. In past studies of the PRFs [4], [5] Curran et al. estimated rate constants for the $\dot{O}_2QOOH \rightleftharpoons HO_2\dot{Q}OOH$ isomerization reactions based on those estimated for $R\dot{O}_2 \rightleftharpoons \dot{Q}OOH$ isomerization reactions, but with a reduced activation energy of 3 kcal mol^{-1} and a frequency factor based on the degeneracy of the number of H-atom available for the reaction. This was because no data (experimental or theoretical) existed for $\dot{O}_2QOOH \rightleftharpoons HO_2\dot{Q}OOH$ isomerization reactions. Previous studies of low temperature ethane and propane chemistry [249] focused on the system $\dot{R} + O_2 \rightarrow R\dot{O}_2 \rightleftharpoons \dot{Q}OOH$ and subsequent propagation reactions of ȮOH radicals but did not include the second hydroperoxyl-alkyl radical addition to O_2 and subsequent steps. A more recent study by Goldsmith et al. [198] studied the second addition to O_2 including the sequence $\dot{O}_2QOOH \rightleftharpoons HO_2\dot{Q}OOH \rightarrow R\dot{O} + \dot{O}H + \dot{O}H$.

Miyoshi [165] and Sharma et al. [197] have also both calculated rate constants for sets of training reactions for $\dot{O}_2QOOH \rightleftharpoons HO_2\dot{Q}OOH$ isomerization reactions using quantum chemistry calculations at the CBS-QB3 level of theory. Sharma et al. proposed an alternative hindered-rotor treatment for $\dot{O}_2QOOH$ radicals, as these molecules are complicated by the fact that they have multiple internal rotors with potentials that are dependent on one another. They found that interactions between oxygen and hydrogen atoms in the molecule result in a lowest energy conformer that has a ring shape, with the peroxyl group forming a hydrogen bond with the –OOH group. Miyoshi [165] did not consider these hindered-rotor interactions. The rate constants calculated by Sharma et al. for reactions which proceed through 5-membered transition state rings are, in general, faster than those calculated by Miyoshi (although those proceeding through the "primary" pathways are roughly equal), whereas reactions proceeding through 6-, 7- and 8-membered rings are generally slower compared to Miyoshi.

5. Conclusions

- Due to increasing computational ability detailed chemical kinetic models for even larger hydrocarbon and oxygenated hydrocarbon molecules are being produced.
- There have been few studies either measuring and/or computing diffusion coefficients for reacting species—the community needs more.
- There has been a lack of focus on accurate thermochemistry for species. The ATcT is a very good start and is a recommended source of heats of formation for the species which are included in it but accurate entropy and heat capacity values are also needed.
- Experimental measurements and high-level quantum chemistry calculations of rate constants for reactions involved in the C_0–C_4 sub-system are vital for accurate predictions of all higher order hydrocarbon and oxygenated hydrocarbon species. A lot has been done in this area but a lot more work still needs to be done.

- Rate rules are useful in the development of detailed kinetic mechanisms. With increasing computational ability rate constants can be calculated at a higher level of theory and for larger molecules than ever before. The community continues to push the bounds of theory and size of molecule that can be studied.

Acknowledgements

I would like to acknowledge Drs Kieran Somers, Ultan Burke, William Pitz, Charles Westbrook, Tiziano Faravelli and Stephen Klippenstein for their help and feedback in preparing this manuscript.

References

[1] M. Frenklach, H. Wang, C.T. Bowman, R.K. Hanson, G.P. Smith, D.M. Golden, W.C. Gardiner Jr, V. Lissianski, 25th Intl. Symp. Combust., (1994) Poster WIP-3-26.

[2] C.T. Bowman, R.K. Hanson, D.F. Davidson, W.C. Gardiner Jr., V. Lissianski, G.P. Smith, D.M. Golden, M. Frenklach, H. Wang, M. Goldenberg, GRI-Mech version 2.11. 1995: available at http://www.me.berkeley.edu/gri_mech.

[3] G.P. Smith, D.M. Golden, M. Frenklach, N.W. Moriarty, B. Eiteneer, M. Goldenberg, C.T. Bowman, R.K. Hanson, S. Song, W.C. Gardiner, Jr., V.V. Lissianski, Z. Qin, available at http://combustion.berkeley.edu/gri-mech/version30/text30.html (accessed December 6 2017).

[4] H.J. Curran, P. Gaffuri, W.J. Pitz, C.K. Westbrook, Combust. Flame 114 (1998) 149–177.

[5] H.J. Curran, P. Gaffuri, W.J. Pitz, C.K. Westbrook, Combust. Flame 129 (2002) 253–280.

[6] C.K. Westbrook, W.J. Pitz, O. Herbinet, H.J. Curran, E.J. Silke, Combust. Flame 156 (2009) 181–199.

[7] C.K. Westbrook, C.V. Naik, O. Herbinet, W.J. Pitz, M. Mehl, S.M. Sarathy, H.J. Curran, Combust. Flame 158(4) (2011) 742–755.

[8] M. Mehl, W.J. Pitz, C.K. Westbrook, H.J. Curran, Proc. Combust. Inst. 33 (2011) 193–200.

[9] S. Dooley, S.H. Won, M. Chaos, J. Heyne, Y. Ju, F.L. Dryer, K. Kumar, C-J. Sung, H. Wang, M.A. Oehlschlaeger, R.J. Santoro, T.A. Litzinger Combust. Flame 157(12) (2010) 2333–2339.

[10] S. Dooley, S.H. Won, J. Heyne, T.I. Farouk, Y. Ju, F.L. Dryer, K. Kumar, X. Hui, C-J. Sung, H. Wang, M.A. Oehlschlaeger, V. Iyer, S. Iyer, T.A. Litzinger, R.J. Santoro, T. Malewicki, K. Brezinsky, Combust. Flame 159(4) (2012) 1444–1466.

[11] F.L. Dryer, Proc. Combust. Inst. 35 (2015) 117–144.

[12] S. Arrhenius, Z. phys. Chem. 4 (1889) 226.

[13] D.M. Kooij, Z. phys. Chem. 12 (1893) 155.

[14] M. Berthdot, Ann. Chim. Phys. 66(3) (1862) 110.

[15] https://www.ansys.com/products/fluids/ansys-chemkin-pro

[16] A. Cuoci, A. Frassoldati, T. Faravelli, E. Ranzi, Combust. Flame 160 (2013) 870–886.

[17] A. Cuoci, A. Frassoldati, T. Faravelli, E. Ranzi, Combust. Flame 156 (2009) 2010–2022.

[18] David G. Goodwin, Harry K. Moffat, and Raymond L. Speth. Cantera: An object-oriented software toolkit for chemical kinetics, thermodynamics, and transport processes. http://www.cantera.org, 2017. Version 2.3.0. doi:10.5281/zenodo.170284 (see: http://www.cantera.org/docs/sphinx/html/about.html#citing-cantera).

[19] D. Goodwin, Cantera: object-oriented software for reacting flows. Technical report. California Institute of Technology; 2005.

[20] LOGEresearch v 1.10 (LOGE AB) - www.logesoft.com/loge-software/

[21] H. Pitsch, A C++ computer program for 0D combustion and 1D laminar flame calculations (1990) http://www.itv.rwth-aachen.de/downloads/flamemaster/.

[22] Computational Modelling Cambridge Ltd. Kinetics: the chemical kinetics model builder https://cmclinnovations.com/products/kinetics/.

[23] O. Deutschmann, S. Tischer, C. Correa, D. Chatterjee, S. Kleditzsch, V.M. Janardhanan, N. Mladenov, H. D. Minh, H. Karadeniz, M. Hettel, DETCHEM Software package, 2.5 ed., www.detchem.com, Karlsruhe 2014.

[24] http://www.rotexo.com/index.php/en/

[25] http://www.kintechlab.com/products/chemical-workbench/

[26] C. Liu, W.S. McGivern, J.A. Manion, H. Wang, J. Phys. Chem. A. 120(41) (2016) 8065–8074.

[27] K. Chae, P. Elvati, A. Violi, J. Phys. Chem. B 115(3) (2011) 500–506.

[28] K. Chae, A. Violi, J. Chem. Phys. 134(4) (2011) 044537.

[29] A.W. Jasper, E. Kamarchik, J.A. Miller, S.J. Klippenstein, J. Chem. Phys. 141(12) (2014) 124313.

[30] A.W. Jasper, J.A. Miller, Combust. Flame 161(1) (2014) 101–110.

[31] J.A. Miller, R.J. Kee, C.K. Westbrook, Annu. Rev. Phys. Chem. 41 (1990) 345–387.

[32] M. Frenklach, H. Wang, M.J. Rabinowitz, Prog. Energy Combust. Sci. 18 (1992) 47–73.

[33] J.M. Simmie, Prog. Energy Combust. Sci. 29 (2003) 599–634.

[34] C.K. Westbrook, Y. Mizobunchi, T.J. Poinsot, P.J. Smith, J. Warnatz, Proc. Combust. Inst. 30 (2005) 125-157.

[35] G.E. Moore, Electronics 38(8) (1965) 114.

[36] T.F. Lu and C.K. Law, Prog. Energy Combust. Sci. 35 (2009) 192–215.

[37] F.N. Egolfopoulos, N. Hansen, Y. Ju, K. Kohse-Höinghaus, C.K. Law, F. Qi, Prog. Energy Combust. Sci. 43 (2014) 36–67.

[38] C.W. Gear, The automatic integration of stiff ordinary differential equations in: A.J.H. Morrell (ed.), Information Processing, North-Holland, Amsterdam, 1969, pp. 187–193.

[39] C.W. Gear, Numerical Initial Value Problems in Ordinary Differential Equations, Prentice-Hall, Englewood Cliffs, NJ, 1971.

[40] J.O. Hirschfelder, C.F. Curtiss, D.E. Campbell, J. Chem. Phys. 57 (1953) 403.

[41] D.B. Spalding, Philos. Trans. R. Soc. Lond. A 249 (1956) 1–25.

[42] D.J. Seery, C.T. Bowman, Combust. Flame 14 (1970) 37–48.

[43] C.T. Bowman, Combust. Sci. Technol. 2 (1970) 161–172.

[44] P.J. Marteney, Combust. Sci. Technol. 1 (1970) 461.

[45] L.D. Smoot, W.C. Hecker, G.A. Williams, Combust. Flame 26 (1976) 323–342

[46] G. Tsatsaronis, Combust. Flame 33 (1978) 217–239.

[47] C.T. Bowman, Combust. Flame 25 (1975) 343–354.

[48] C.K. Westbrook, F.L. Dryer, Combust. Sci. Technol. 20 (1979) 125–140.

[49] C.K. Westbrook, F.L. Dryer, Proc. Combust. Inst. 18 (1980) 749–767.

[50] C.K. Westbrook, F.L. Dryer, Prog. Energy Combust. Sci. 10 (1984) 1–57.

[51] J. Warnatz, Intl. Symp. Combust. 18 (1981) 369–384.

[52] J. Warnatz, Combust. Sci. Technol. 34 (1983) 177–200.

[53] P. Dagaut, J.C. Boettner, M. Cathonnet, Comb. Sci. Technol. 77 (1991) 127–148.

[54] P. Dagaut, J.C. Boettner, M. Cathonnet, Int. J. Chem. Kinet. 23 (1991) 437–455.

[55] Y. Tan, P. Dagaut, M. Cathonnet, J.C. Boettner, J.S. Bachman, P. Carlier, Proc. Combust. Inst. 25 (1994) 1563–1569.

[56] P. Barbé, F. Battin-Leclerc, G.M. Côme, J. Chim. Phys. 92 (1995) 1666–1692.

[57] K.J. Hughes, T. Turányi, A.R. Clague, M. Pilling, J. Int. J. Chem. Kinet. 33 (2001) 513–538.

[58] J.A. Miller, C.T. Bowman, Prog. Energy Combust. Sci. 15 (1989) 287–338.

[59] R.A. Yetter, F.L. Dryer, H. Rabitz, Combust. Sci. Technol. 79 (1991) 97–128.

[60] S. Hochgreb, F.L. Dryer, Combust. Flame 91 (1992) 257–284.

[61] T.J. Held, F.L. Dryer, Int. J. Chem. Kinet. 30 (1998) 805–830.

[62] J. Li, Z. Zhao, A. Kazakov, M. Chaos, F.L. Dryer, J.J. Scire, Int. J Chem. Kinet. 39 (2007) 109–136.

[63] M. Frenklach, Combust Flame 58 (1984) 69–72.

[64] http://web.eng.ucsd.edu/mae/groups/combustion/mechanism.html

[65] J.C. Prince, F.A. Williams, Combust Flame 159 (2012) 2336–2344.

[66] H. Wang, X. You, A.V. Joshi, S.G. Davis, A. Laskin, F. Egolfopoulos, C.K. Law, USC Mech Version II. High-Temperature Combustion Reaction Model of H2/CO/C1–C4 Compounds. http://ignis.usc.edu/USC_Mech_II.htm, May 2007.

[67] H. Wang, E. Dames, B. Sirjean, D.A. Sheen, R. Tango, A. Violi, J.Y.W. Lai, F.N. Egolfopoulos, D.F. Davidson, R.K. Hanson, C.T. Bowman, C.K. Law, W. Tsang, N.P. Cernansky, D.L. Miller, R.P. Lindstedt, A high-temperature chemical kinetic model of n-alkane (up to n-dodecane), cyclohexane, and methyl-, ethyl-, n-propyl and n-butyl-cyclohexane oxidation at high temperatures, JetSurF version 2.0, September 19, 2010 (http://web.stanford.edu/group/haiwanglab/JetSurF/JetSurF2.0/index.html).

[68] E. Ranzi, A. Frassoldati, R. Grana, A. Cuoci, T. Faravelli, A.P. Kelley, C.K. Law, Prog. Energy Combust. Sci., 38(4) (2012) 468–501.

[69] http://creckmodeling.chem.polimi.it/

[70] W.K. Metcalfe, S.M. Burke, S.S. Ahmed, H.J. Curran, Int. J. Chem. Kinet. 45 (2013) 638–675.

[71] Y. Li, C-W. Zhou, K.P. Somers, K. Zhang, H.J. Curran, Proc. Combust. Inst. 36(1) (2017) 403–411.

[72] C-W. Zhou, Y. Li, E. O'Connor, K.P. Somers, S. Thion, C. Keesee, O. Mathieu, E.L. Petersen, T. A. DeVerter, M.A. Oehlschlaeger, G. Kukkadapu, C-J. Sung, M. Alrefae, F. Khaled, A. Farooq, P. Dirrenberger, P-A. Glaude, F. Battin-Leclerc, J. Santner, Y. Ju, T. Held, F.M. Haas, F.L. Dryer, H.J. Curran, Combust. Flame 167 (2016) 353–379.

[73] J. Gimenez-Lopez, C.T. Rasmussen, H. Hashemi, M.U. Alzueta, Y. Gao, P. Marshall, C.F. Goldsmith, P. Glarborg, Int. J. Chem. Kinet. 48 (2016) 724–738.

[74] N. Cohen, R.K. Westberg, J. Phys. Chem. Ref. Data 12 (1983) 531–590.

[75] N. Cohen, R.K. Westberg, J. Phys. Chem. Ref. Data 20 (1991), 1211–1311.

[76] W. Tsang, R.F. Hampson, J. Phys. Chem. Ref. Data 15 (1986) 1087–1279.

[77] W. Tsang, J. Phys. Chem. Ref. Data 16 (1987) 471–508.

[78] W. Tsang, J. Phys. Chem. Ref. Data 17 (1988) 887–951.

[79] W. Tsang, J. Phys. Chem. Ref. Data 19 (1990) 1–68.

[80] W. Tsang, J. Phys. Chem. Ref. Data 20 (1991) 221–273.

[81] D.L. Baulch, C.J. Cobos, R.A. Cox, C. Esser, P. Frank, T. Just, J.A. Kerr, M.J. Pilling, J. Troe, R.W. Walker, J. Warnatz, J. Phys. Chem. Ref. Data 21 (1992) 411–736.

[82] D.L. Baulch, C.J. Cobos, R.A. Cox, P. Frank, G.D. Hayman, T. Just, J.A. Kerr, T.P. Murrells, M.J. Pilling, J. Troe, R.W. Walker, J. Warnatz, Combust. Flame 98 (1994) 59–79.

[83] D.L. Baulch, C.T. Bowman, C.J. Cobos, R.A. Cox, T. Just, J.A. Kerr, M.J. Pilling, D. Stocker, J. Troe, W. Tsang, R.W. Walker, J. Warnatz, J. Phys. Chem. Ref. Data 34 (2005) 757–1397.

[84] NIST Chemical Kinetics Database, Standard Reference Database 17 http://kinetics.nist.gov/kinetics/index.jsp.

[85] S. Dooley, H.J. Curran, J.M. Simmie, Combust. Flame 153 (2008) 2–32.

[86] J.F. Griffiths, J.A. Barnard, in Flame and Combustion. 3rd ed. Blackie Academic & Professional/Chapman & Hall, New York, NY (1995).

[87] W. Liang, C.K. Law, Phys. Chem. Chem. Phys. 20 (2018) 742–751.

[88] A. Kéromnès, W.K. Metcalfe, K.A. Heufer, N. Donohoe, A.K. Das, C.J. Sung, J. Herzler, C. Naumann, P. Griebel, O. Mathieu, M.C. Krejci, E.L. Petersen, W.J. Pitz, H.J. Curran, Combust. Flame 160 (2013) 995–1011.

[89] J. Li, Z. Zhao, A. Kazakov, F.L. Dryer, Int. J. Chem. Kinet. 36 (2004) 566–575.

[90] M.P. Burke, M. Chaos, Y. Ju, F.L. Dryer, S.J. Klippenstein, Int. J. Chem. Kinet. 44 (2012) 444–474.

[91] H. Hashemi, J.M. Christensen, S. Gersen, P. Glarborg, Proc. Combust. Inst. 35 (2015) 553–560.

[92] M.P. Burke, S.J. Klippenstein, L.B. Harding, Proc. Combust. Inst. 34 (2013) 547–555.

[93] M. Sangwan, L.N. Krasnoperov, J. Phys. Chem. A 116 (2012) 11817–11822.

[94] D.D.Y. Zhou, K. Han, P. Zhang, L.B. Harding, M.J. Davis, R.T. Skodje, J. Phys. Chem. A 116 (2012) 2089–2100.

[95] T. Varga, T. Nagy, C. Olm, I. Gy. Zsély, R. Pálvölgyi, E. Valkó, G. Vincze, M. Cserháti, H.J. Curran, T. Turányi, Proc. Combust. Inst. 35 (2015) 589–596.

[96] T. Turányi, T. Nagy, I. Gy. Zsély, M. Cserháti, T. Varga, B. Szabó, I. Sedyó, P.T. Kiss, A. Zempléni, H.J. Curran, Int. J. Chem. Kinet. (2012) 44 284–302.

[97] D. Miller; M. Frenklach, Int. J. Chem. Kinet. 15 (1983) 677-696

[98] M. Frenklach, Combust. Flame 58 (1984) 69–72.

[99] M. Frenklach; D. Miller, AIChE J. 31 (1985) 498–500.

[100] R. Feeley; P. Seiler; A. Packard; M. Frenklach, J. Phys. Chem. A 108 (2004) 9573–9583.

[101] R. Feeley; M. Frenklach; M. Onsum; T. Russi; A. Arkin; A. Packard, J. Phys. Chem. A 110 (2006) 6803–6813.

[102] M. Frenklach, Proc. Combust. Inst. 31 (2007) 125–140.

[103] X.Q. You; A. Packard; M. Frenklach, Int. J. Chem. Kinet. 44 (2012) 101–116.

[104] P. Seiler; M. Frenklach; A. Packard; R. Feeley, Optim. Eng. 7 (2006) 459–478.

[105] PrIMe, Web site http://www.primekinetics.org/)

[106] Z. Qin, V. Lissianski, H. Yang, W. Gardiner, S. Davis, H. Wang, Proc. Combust. Inst. 28 (2000) 1663–1669.

[107] S.G. Davis, A.V. Joshi, H. Wang, F.N. Egolfopoulos, Proc. Combust. Inst. 30 (2005) 1283–1292.

[108] D.A. Sheen, X. You, H. Wang, T. Løvås, Proc. Combust. Inst. 32 (2009) 535–542.

[109] X.Q. You, T. Russi, A. Packard, M. Frenklach, Proc. Combust. Inst. 33 (2011) 509–516.

[110] D.A. Sheen, H. Wang, Combust Flame 158 (2011) 645–656.

[111] J.J. Scire, F.L. Dryer, R.A. Yetter, Int. J. Chem. Kinet. 33(12) (2001) 784–802.

[112] C. Olm, T. Varga, É. Valkó, H.J. Curran, T. Turányi, Combust. Flame 186 (2017) 45–64.

[113] C. Olm, T. Varga, É. Valkó, S. Hartl, C. Hasse, T. Turányi, Int. J. Chem. Kinet. 48 (2016) 423–441.

[114] M.S. Bernardi, M. Pelucchi, A. Stagni, L.M. Sangalli, A. Cuoci, A. Frassoldati, P. Secchi, T. Faravelli, Combust. Flame 168 (2016) 186–203.

[115] C. Olm, I. Gy. Zsély, R. Pálvölgyi, T. Varga, T. Nagy, H.J. Curran, T. Turányi, Combust. Flame 161 (2014) 2219–2234.

[116] C. Olm, I. Gy. Zsély, T. Varga, H. J. Curran, T. Turányi, Combust. Flame 162 (2015) 1793–1812.

[117] M.P. Burke, S.J. Klippenstein, L.B. Harding, Proc. Combust. Inst. 34 (2013) 547–555.

[118] M.P. Burke, C.F. Goldsmith, S.J. Klippenstein, O. Welz, H. Huang, I.O. Antonov, J.D. Savee, D.L. Osborn, J. Zádor, C.A. Taatjes, L. Sheps, J. Phys. Chem. A 119 (2015) 7095–7115.

[119] J. Zádor, H.N. Najm "Automated exploration of the mechanism of elementary reactions (SAND2012-8095)," Sandia National Laboratories, 2012.

[120] J. Zádor, J.A. Miller, Proc. Combust. Inst. 35 (2015) 181–188.

[121] M. Keceli, S. Elliott, Y-P. Li, M.S. Johnson, C. Cavallotti, Y. Georgievskii, W.H. Green, M. Pelucchi, J.M. Wozniak, A.W. Jasper, S.J. Klippenstein, Proc. Combust. Inst. 37 (2019) accepted.

[122] ReSpecTh, webpage. http://respecth.hu.

[123] T. Varga, T. Turányi, E. Czinki, T. Furtenbacher, A.G. Császár, Proc. ECM2015 (2015) Paper P1-04.

[124] B.W. Weber, K.E. Niemeyer, Int. J. Chem. Kinet. 50(3) (2018) 135–148.

[125] J. Bugler, B. Marks, O. Mathieu, R. Archuleta, A. Camou, C. Grégoire, K.A. Heufer, E.L. Petersen, H.J. Curran, Combust. Flame 163(1) (2016) 138–156.

[126] C.K. Westbrook, H.J. Curran, W.J. Pitz, J.F. Griffiths, C. Mohamed, S.K. Wo, Proc. Combust. Inst. 27(1) (1998) 371–378.

[127] A. Yamamoto, H. Oshibe, H. Nakamura, T. Tezuka, S. Hasegawa, K. Maruta, Proc. Combust. Inst. 33 (2011) 3259–3266.

[128] C.K. Westbrook, Proc. Combust. Inst. 28 (2000) 1563–1577.

[129] S.J. Klippenstein, Y. Georgievskii, L.B. Harding, Proc. Combust. Inst. 29 (2002) 1229–1236.

[130] L.B. Harding, Y. Georgievskii, S.J. Klippenstein, J. Phys. Chem. A 109 (2005) 4646–4656.

[131] J. Troe, J. Phys. Chem. 83 (1979) 114–126.

[132] A.W. Jasper, J.A. Miller, J. Phys. Chem. A 115 (2011) 6438–6455.

[133] W. Lowry, J. de Vries, M. Krejci, E. Petersen, Z. Serinyel, W. Metcalfe, H. Curran, G. Bourque, J. Eng. Gas Turbines Power 133 (2011) 091501.

[134] X.J. Gu, M.Z. Haq, M. Lawes, R. Woolley, Combust Flame 121 (2000) 41–58.

[135] G. Rozenchan, D.L. Zhu, C.K. Law, S.D. Tse, Proc. Combust. Inst. 29 (2002) 1461–1469.

[136] J.A. Miller, A.E. Lutz, personal communication, August 2003.

[137] N. Marinov, W. Pitz, C. Westbrook, A. Vincitore, M. Castaldi, S. Senkan, C. Melius, Combust. Flame 114 (1998) 192–213.

[138] I.R. Slagle, J.-Y. Park, M.C. Heaven, D. Gutman, J. Am. Chem. Soc. 106 (1984) 4356–4361.

[139] P.R. Westmoreland, Combust. Sci. Tech. 82 (1992) 151–168.

[140] J.W. Bozzelli, A.M. Dean, J. Phys. Chem. 97 (1993) 4427–4441.

[141] B.K. Carpenter, J. Phys. Chem. 99 (1995) 9801–9810.

[142] A.M. Mebel, E.W.G. Diau, M.C. Lin, K. Morkuma, J. Am. Chem. Soc. 118 (1996) 9759–9771.

[143] C.F. Goldsmith, L.B. Harding, Y. Georgievskii, J.A. Miller, S.J. Klippenstein, J. Phys. Chem. A 119 (2015) 7766–7779.

[144] S.J. Klippenstein, Proc. Combust. Inst. 36 (2017) 77–111.

[145] N. Lokachari, U. Burke, A. Ramalingam, M. Turner, H. Hesse, K.P. Somers, J. Beeckmann, K.A. Heufer, E.L. Petersen, H.J. Curran, Proc. Combust. Inst. 37 (2019) accepted.

[146] J. Gimenez-Lopez, C.T. Rasmussen, H. Hashemi, M.U. Alzueta, Y. Gao, P. Marshall, C.F. Goldsmith, P. Glarborg, Int. J. Chem. Kinet. 48 (2016) 724–738.

[147] E. Ranzi, M. Dente, S. Pierucci, G. Biardi, Ind. Eng. Chem. Fundam. 22 (1983) 132–139.

[148] M. Dente, E Ranzi, L. Albright, Bryce, Corcoran (Eds.), Pyrolysis theory and industrial practice, Academic Press, San Diego (1983) (Chapter 7).

[149] http://www.spyrosuite.com/pyrotec/history/

[150] E. Ranzi, T. Faravelli, P. Gaffuri, G. Pennati, Combust. Flame 102 (1995) 179–192.

[151] E.I. Axelsson, K. Brezinsky, F.L. Dryer, W.J. Pitz, C.K. Westbrook, Proc. Combust. Inst. 21 (1986) 783–793.

[152] J. Warnatz, Proc. Combust. Inst. 20 (1984) 845–856.

[153] T.J. Held, A.J. Marchese, F.L. Dryer, Combust. Sci. Tech. 123 (1997) 107–146.

[154] R. Xu, K. Wang, S. Banerjee, J.K. Shao, T. Parise, Y. Zhu, S. Wang, A. Movaghar, D.J. Lee, R. Zhao, X. Han, Y. Gao, T. Lu, K. Brezinsky, F.N. Egolfopoulos, D.F. Davidson, R.K. Hanson, C.T. Bowman, H. Wang, Combust. Flame (2018) doi.org/10.1016/j.combustflame.2018.03.021.

[155] G.E. Quelch, M.M. Gallo, M. Shen, Y. Xie, H.F. Schaefer III, D. Moncrieff, J. Am. Chem. Soc. 116 (1994) 4953–4962.

[156] R.R. Baldwin, C.E. Dean, R.W. Walker, J. Chem. Soc. Faraday Trans. 82 (1986) 1445–1455.

[157] K.G. McAdam, R.W. Walker, J. Chem. Soc. Faraday Trans. 83 (1987) 1509–1517.

[158] J.A. Miller, S.J. Klippenstein, Int. J. Chem. Kinet. 33 (2001) 654–668.

[159] J.A. Miller, S.J. Klippenstein, S.H. Robertson, Proc. Combust. Inst. 28 (2000) 1479–1486.

[160] J.C. Rienstra-Kiracofe, W.D. Allen, H.F. Schaefer III, J. Phys. Chem. A 104 (2000) 9823–9840.

[161] E.P. Clifford, J.T. Farrell, J.D. DeSain, C.A. Taatjes, J. Phys. Chem. A. 104 (2000) 11549–11560.

[162] E.G. Estupiñán, J.D. Smith, A. Tezaki, L.E. Jusinski, S.J. Klippenstein, C.A. Taatjes, J. Phys. Chem. A 111 (2007) 4015–4030.

[163] S.M. Villano, L.K. Huynh, H.H. Carstensen, A.M. Dean, J. Phys. Chem. A 115 (2011) 13425–13442.

[164] S.M. Villano, L.K. Huynh, H.H. Carstensen, A.M. Dean, J. Phys. Chem. A 116 (2012) 5068–5089.

[165] A. Miyoshi, J. Phys. Chem. A 115 (2011) 3301–3325.

[166] A. Miyoshi, A. Int. J. Chem. Kinet. 44 (2012) 59–74.

[167] A.A. Jemi-Alade, P.D. Lightfoot, R. Lesclaux, Chem. Phys. Lett. 195 (1992) 25–30.

[168] R.R. Baldwin, R.W. Walker, Proc. Combust. Inst. 17 (1979) 525–533.

[169] R.W. Walker, C. Morley, in *Comprehensive Chem. Kinetics* (M. J. Pilling, Ed.), Elsevier, Amsterdam, 35:1 (1997).

[170] M. Scott, R.W. Walker, Combust. Flame 129 (2002) 365–377.

[171] M. Blocquet, C. Schoemaecker, D. Amedro, O. Herbinet, F. Battin-Leclerc, C. Fittschen, Proc. Natl. Acad. Sci. U. S. A. 110 (2013) 20014–20017.

[172] B. Brumfield, W.T. Sun, Y. Wang, Y. Ju, G. Wysocki, Opt. Lett. 39 (2014) 1783–1786.

[173] N. Kurimoto, B. Brumfield, X. Yang, T. Wada, P. Diévart, G. Wysocki, Y. Ju, Proc. Combust. Inst. 35(1) (2015) 457–464.

[174] M. Djehiche, N.L. Le Tan, C.D. Jain, G. Dayma, P. Dagaut, C. Chauveau, L. Pillier, A. Tomas, J. Am. Chem. Soc. 136 (2014) 16689–16694.

[175] H.-H. Carstensen, A.M. Dean, Proc. Combust. Inst. 30 (2005) 995–1003.

[176] H.-H. Carstensen, A.M. Dean, O. Deutschmann, Proc. Combust. Inst. 31 (2007) 149–157.

[177] J. Aguilera-Iparraguirre, H.J. Curran, W. Klopper, J.M. Simmie, J. Phys. Chem. A 112 (2008) 7047–7054.

[178] J. Mendes, C.-W. Zhou, H.J. Curran, J. Phys. Chem. A 118(51) (2014) 12089–12104.

[179] J. Mendes, C-W. Zhou, H.J. Curran, J. Phys. Chem. A 118(8) (2014) 1300–1308.

[180] J. Mendes, C-W. Zhou, H.J. Curran, J. Phys. Chem. A 117(51) (2013) 14006–14018.

[181] J. Mendes, C-W. Zhou, H.J. Curran, J. Phys. Chem. A 117(22) (2013) 4515–4525.

[182] C-W. Zhou, J.M. Simmie, H.J. Curran, Int. J. Chem. Kinet. 44 (2012) 155–164.

[183] M. Altarawneh, A.H. Al-Muhtaseb, B.Z. Dlugogorski, E.M. Kennedy, J.C. Mackie, J. Comp. Chem. 32 (2011) 1725–1733.

[184] I.M. Alecu, D.G. Truhlar, J. Phys. Chem. A 115 (2011) 14599–14611.

[185] S.J. Klippenstein, L.B. Harding, M.J. Davis, A.S. Tomlin, R.T. Skodje, Proc. Combust. Inst. 33 (2011) 351–357.

[186] C. Olm, T. Varga, É Valkó, H.J. Curran, T. Turányi, Combust. Flame 186 (2017) 45–64.

[187] U. Burke, W.K. Metcalfe, S.M. Burke, K.A. Heufer, P. Dagaut, H.J. Curran, Combust. Flame 165 (2016) 125–136.

[188] U. Burke, K.P. Somers, P. O'Toole, C.M. Zinner, N. Marquet, G. Bourque, E.L. Petersen, W.K. Metcalfe, Z. Serinyel, H.J. Curran, Combust. Flame 162(2) (2015) 315–330.

[189] J.H. Knox in: P.G. Ashmore, T.M. Sugden, F.S. Dainton, editors. Photochemistry and reaction kinetics. Cambridge: Cambridge University Press; 1967.

[190] A. Fish, Oxidation of Organic Compounds, Vol. 2. Adv. Chem. Ser. 76 (1968) 58.

[191] R.T. Pollard, Hydrocarbons. In: C.H. Bamford, C.F.H. Tipper editors. Comprehensive Chemical Kinetics: Gas Phase Combustion, vol. 17. Amsterdam: Elsevier; 1977.

[192] R.A. Cox, J.A. Cole, Combust. Flame, 60 (1985) 109–123.

[193] H. Hu, J.C. Keck, SAE J. (1987) SAE-872210.

[194] R.W. Walker, C. Morley, Basic Chemistry of Combustion. In: M. J. Pilling, editor. Comprehensive Chemical Kinetics: Low-Temperature Combustion and Autoignition, vol. 35. Amsterdam: Elsevier; 1997.

[195] J.F. Griffiths, Prog. Energy Combust. Sci. 21 (1995) 25–107.

[196] J. Zádor, C.A. Taatjes, R.X. Fernandes, Prog. Energy Combust. Sci. 37 (2011) 371–421.

[197] S. Sharma, S. Raman, W.H. Green, J. Phys. Chem. A 114 (2010) 5689–5701.

[198] C.F. Goldsmith, W.H. Green, S.J. Klippenstein, J. Phys. Chem. A 116 (2012**)** 3325–3346.

[199] Z. Wang, D.M. Popolan-Vaida, B. Chen, K. Moshammer, S. Mohamed, H. Wang, S. Sioud, M.A. Raji, K. Kohse-Höinghaus, N. Hansen, P. Dagaut, S.R. Leone, S.M. Sarathy. Proc. Natl. Acad. Sci. 114(50) (2017) 13102–13107.

[200] Z. Wang, B. Chen, K. Moshammer, D.M. Popolan-Vaida, S. Sioud, V.S. Bhavani Shankar, D. Vuilleumier, T. Tao, L. Ruwe, E. Bräuer, N. Hansen, P. Dagaut, K. Kohse-Höinghaus, M.A. Raji, S.M. Sarathy. Combust. Flame 187 (2018) 199–216.

[201] J. Bugler, K.P. Somers, E.J. Silke, H.J. Curran, J. Phys. Chem. A 119(28) (2015) 7510–7527.

[202] J. Bugler, A. Rodriguez, O. Herbinet, F. Battin-Leclerc, P. Dagaut, H.J. Curran, Proc. Combust. Inst. 36(1) (2017) 441–448.

[203] S.M. Burke, J.M. Simmie, H.J. Curran, J. Phys. Chem. Ref. Data 44 (2015) 013101.

[204] L. Cai, H. Pitsch, S.Y. Mohamed, V. Raman, J. Bugler, H. Curran, S.M. Sarathy, Combust. Flame (2016) 173:468–482.

[205] N. Atef, G. Kukkadapu, S.Y. Mohamed, M. Al Rashidi, C. Banyon, M. Mehl, A. Heufer, E.F. Nasir, A. Alfazazia, A.K. Das, C.K. Westbrook, W.J. Pitz, T. Lu, A. Farooq, C-J. Sung, H.J. Curran, S.M. Sarathy, Combust. Flame 178 (2017) 111–134.

[206] E. Christensen, J. Yanowitz, M. Ratcliff, R.L. McCormick, Energy Fuels 25 (2011) 4723–4733.

[207] Fuels and Lubricants Handbook: Technology, Properties, Performance, and Testing (Astm Manual Series, Mnl 37). George E. Totten, editor; Section editors, Steven R. Restbrook, Rajesh J. Shah. ISBN 0-8031-2096-6.

[208] S.M. Sarathy, P. Oßwald, N. Hansen, K. Kohse-Höinghaus, Prog. Energy Combust. Sci. 44 (2014) 40–102.

[209] G. da Silva, J.W. Bozzelli, L. Liang, J.T. Farrell, J. Phys. Chem. A 113 (2009) 8923–8933.

[210] S.M. Sarathy, S. Vranckx, K. Yasunaga, M. Mehl, P. Oßwald, W.K. Metcalfe, C.K. Westbrook, W.J. Pitz, K. Kohse-Höinghaus, R. Fernandes, H.J. Curran, Combust. Flame 159(6) (2012) 2028–2055.

[211] M.P. Halstead, L.J. Kirsch, A. Prothero, C.P. Quinn, Proc. R. Soc. London A 346 (1975) 515–538.

[212] E. Ranzi, P. Gaffuri, T. Faravelli, P. Dagaut, Combust. Flame 103 (1995) 91–106.

[213] E. Ranzi, T. Faravelli, P. Gaffuri, A. D'Anna A. Ciajola, Combust. Flame 108 (1997) 24–42.

[214] C. Chevalier, J. Warnatz, H. Melenk, Bes. Bun. Phys. Chem. 94 (1990) 1362–1367.

[215] C. Chevalier, W.J. Pitz, J. Warnatz, C.K. Westbrook, H. Melenk, Proc. Combust. Inst. 24 (1992) 93–101.

[216] M. Nehse, J. Warnatz, C. Chevalier, Proc. Combust. Inst. 26 (1996) 773–780.

[217] C. Morley, Proc. Anglo German Combustion Symp., Queen's College, Cambridge, 1993.

[218] E.S. Blurock, J. Chem. Inf. Comput. Sci. 35 (1995) 607–616.

[219] G. Moréac, E.S. Blurock, F. Mauss, Combust. Sci. Tech. 178 (2006) 2025–2038.

[220] F. Buda, R. Bounaceur, V. Warth, P.-A. Glaude, R. Fournet, F. Battin-Leclerc, Combust. Flame 142 (2005) 170–186.

[221] L. Haux, P.Y. Cunin, M. Griffiths, G.M. Côme, J. Chim. Phys. 82 (1985) 1027–1031.

[222] L. Haux, P.Y. Cunin, M. Griffiths, G.M. Côme, J. Chim. Phys. 85 (1988) 739–743.

[223] V. Warth, N. Stef, P.-A. Glaude, F. Battin-Leclerc, G. Scacchi, G.M. Côme, Combust. Flame 114 (1998) 81–102.

[224] C. Muller, V. Michel, G. Scacchi, G.M. Côme, J. Chem. Phys. 92 (1995) 1154–1177.

[225] N.M. Vandewiele, K.M. Van Geem, M.F. Reyniers, G.B. Marin, Chem. Eng. J. 207 (2012) 526–538.

[226] R. Van de Vijver, N.M. Vandewiele, A.G. Vandeputte, K.M. Van Geem, M.F. Reyniers, W.H. Green, G.B. Marin, Chem. Eng. J. 278 (2015) 385–393.

[227] S.W. Benson, Thermochemical Kinetics, John Wiley & Sons, New York, 1976.

[228] http://reactionmechanismgenerator.github.io/RMG-Py/index.html

[229] D. Weininger, A. Weininger, J.L. Weininger, J. Chem. Inf. Comput. Sci. 29 (989) 97–101.

[230] https://www.iupac.org/publications/ci/2006/2806/4_tools.html

[231] S. Heller, A. McNaught, S. Stein, D. Tchekhovskoi, I. Pletnev, J. Cheminfo. 5 (1) (2013) 7.

[232] http://support.cas.org/content/chemical-substances

[233] E.R. Ritter, J.W. Bozzelli, Int. J. Chem. Kinet. 23 (1991) 767–778.

[234] http://webbook.nist.gov/chemistry/grp-add/ (retrieved January 12, 2018).

[235] http://www.molknow.com/Online/Estimation.htm

[236] T. Turányi, L. Zalotai, S. Dóbé, T. Bérces, Phys. Chem. Chem. Phys. 4(12) (2002) 2568–2578.

[237] K.J. Hughes, J.F. Griffiths, M. Fairweather, A.S. Tomlin, Phys. Chem. Chem. Phys. 8(27) (2006) 3197–3210.

[238] T. Ziehn, A.S. Tomlin, Int. J. Chem. Kinet., 40 (2008) 742–753.

[239] S.M. Burke, W.K. Metcalfe, O. Herbinet, F. Battin-Leclerc, F.M. Haas, J. Santner, F.L. Dryer, H.J. Curran, Combust. Flame 161(11) (2014) 2765–2784.

[240] S.M. Burke, U. Burke, O. Mathieu, I. Osorio, C. Keesee, A. Morones, E. Petersen, W. Wang, T. DeVerter, M. Oehlschlaeger, B. Rhodes, R. Hanson, D. Davidson, B. Weber, C-J. Sung, J. Santner, Y. Ju, F. Haas, F. Dryer, E. Volkov, E. Nilsson, A. Konnov, M. Alrefae, F. Khaled, A. Farooq, P. Dirrenberger, P-A. Glaude, F. Battin-Leclerc, H.J. Curran, Combust. Flame 162(2) (2015) 296–314.

[241] http://webbook.nist.gov/chemistry/ (retrieved January 12, 2018).

[242] http://www.dlr.de/vt/en/desktopdefault.aspx/tabid-7603/12862_read-32379/ (retrieved January 12, 2018).

[243] https://atct.anl.gov/ (retrieved January 12, 2018).

[244] B. Ruscic, R.E. Pinzon, M.L. Morton, G. von Laszewski, S. Bittner, S.G. Nijsure, K.A. Amin, M. Minkoff, A.F. Wagner, J. Phys. Chem. A 108 (2004) 9979–9997.

[245] B. Ruscic, R.E. Pinzon, G. von Laszewski, D. Kodeboyina, A. Burcat, D. Leahy, D. Montoya, A.F. Wagner, J. Phys. Conf. Ser. 16 (2005) 561–570.

[246] B. Ruscic, Int. J. Quantum Chem. 114 (2014) 1097–1101.

[247] B. Ruscic, J. Phys. Chem. A 119 (2015) 7810–7837.

[248] S. J. Klippenstein, L. B. Harding, B. Ruscic, J. Phys. Chem. A 121 (2017) 6580–6602.

[249] J.D. DeSain, S.J. Klippenstein, J.A. Miller, C.A. Taatjes, J. Phys. Chem. A 107 (2003) 4415–4427.

[250] F.P. Tully, M.L. Koszykowski, J.S. Binkley, Proc. Combust. Inst. 23 (1984) 715–721.

[251] F.P. Tully, A.T. Droege, M.L. Koszykowski, C.F. Melius, J. Phys. Chem. 90 (1986) 691–698.

[252] A.T. Droege, F.P. Tully, J. Phys. Chem. 90 (1986) 1949–1954.

[253] F.P. Tully, J.E.M. Goldsmith, A.T. Droege, J. Phys. Chem. 90 (1986) 5932–5937.

[254] A.T. Droege, F.P. Tully, J. Phys. Chem. 90 (1986) 5937–5941.

[255] J.F. Bott, N. Cohen, Int. J. Chem. Kinet. 16 (1984) 1557–1566.

[256] J.F. Bott, N. Cohen, Int. J. Chem. Kinet. 21 (1989) 485–498.

[257] J.F. Bott, N. Cohen, Int. J. Chem. Kinet. 23 (1991) 1075–1094.

[258] I.B. Koffend, N. Cohen, Int. J. Chem. Kinet. 28 (1996) 79–87.

[259] J. Badra, E.F. Nasir, A. Farooq, J. Phys. Chem. A 118(26) (2014) 4652–4660.

[260] J. Badra, A. Farooq, Combust. Flame 162(5) (2015) 2034–2044.

[261] D. Liu, F. Khaled, B.R. Giri, E. Assaf, C. Fittschen, A. Farooq, J. Phys. Chem. A 121(5) (2017) 927–937.

[262] N. Cohen, Int. J. Chem. Kinet. 23 (1991) 397–417.

[263] R. Sivaramakrishnan, J.V. Michael, J. Phys. Chem. A 113 (2009) 5047–5060.